Journal of Medicinal Chemistry

Article

A Structure-Activity Analysis of Biased Agonism at the Dopamine D2 Receptor

Jeremy Shonberg, Carmen Klein Herenbrink, Laura Lopez Munoz, Arthur Christopoulos, Peter J. Scammells, Ben Capuano, and J. Robert Lane

J. Med. Chem., **Just Accepted Manuscript** • Publication Date (Web): 19 Oct 2013

Journal of Medicinal Chemistry is published by the American Chemical Society. 1155 Sixteenth Street N.W., Washington, DC 20036

A Structure-Activity Analysis of Biased Agonism at the Dopamine D_2 Receptor

Jeremy Shonberg,[†,#] *Carmen Klein Herenbrink,*[‡,#] *Laura López,*[‡] *Arthur Christopoulos,*[‡] *Peter J. Scammells,*[†] *Ben Capuano,*[†,*] *J. Robert Lane.*[‡,*]

[†]Medicinal Chemistry and [‡]Drug Discovery Biology, Monash Institute of Pharmaceutical Sciences, Monash University (Parkville Campus), 381 Royal Parade, Parkville, Victoria 3052 Australia

Abstract

Biased agonism offers an opportunity for the medicinal chemist to discover pathway-selective ligands for GPCRs. A number of studies have suggested that biased agonism at the dopamine D_2 receptor (D_2R) may be advantageous for the treatment of neuropsychiatric disorders, including schizophrenia. As such, it is of great importance to gain insight into the SAR of biased agonism at this receptor. We have generated SAR based around a novel D_2R partial agonist, *tert*-butyl (*trans*-4-(2-(3,4-dihydroisoquinolin-2(1*H*)-yl)ethyl)cyclohexyl)carbamate (**4**). This ligand shares structural similarity to cariprazine (**2**), a drug awaiting FDA approval for the treatment of schizophrenia, yet displays a distinct bias towards two different signaling endpoints. We synthesized a number of derivatives of **4** with subtle structural modifications, including incorporation of cariprazine fragments. By combining pharmacological profiling with analytical methodology to identify and quantify bias we have demonstrated that efficacy and biased agonism can be finely tuned by minor structural modifications to the head group containing the tertiary amine, a tail group that extends away from this moiety and the orientation and length of a spacer region between these two moieties.

Introduction

G protein-coupled receptors (GPCRs), also known as 7-transmembrane receptors are the single largest class of drug targets,[1] and have more than 800 members in the human genome.[2,3] For decades, studies of novel GPCR-targeting compounds have focused almost exclusively on affinity for the receptor as a single descriptor, yet it is efficacy that ultimately determines the nature of the cellular response.[4] More recently, it has become obvious that rather than "linear" (sequentially-coupled) signaling cascades, GPCRs activate non-linked ensembles of G protein-dependent and -independent signaling pathways.[5] Furthermore, there is increasing evidence that highlights the ability of ligands acting at the same GPCR to stabilize distinct receptor conformations that, in turn, are linked to different functional outcomes.[4,6] This challenges earlier ideas of linear efficacy, and the emerging paradigm has been termed biased agonism, stimulus bias, ligand directed signaling, or functional selectivity.[4-8] Biased agonism provides the opportunity to design pathway-selective in addition to receptor subtype selective ligands. However, understanding the structure-activity relationships (SAR) around biased ligands is, as yet, a largely unexplored challenge. To achieve this, standard SAR must be enriched through incorporation of parameters that allow quantification of bias. This concept represents a challenge in itself.

The dopamine D_2 receptor (D_2R) represents a significant drug target for the treatment of diseases including schizophrenia and Parkinson's disease.[9] Currently, all clinically marketed antipsychotics act by targeting the D_2R either as antagonists/inverse agonists (1st and 2nd generation antipsychotics), or partial agonists (3rd generation antipsychotics), thereby modulating the action of the neurotransmitter dopamine. This latter approach is exemplified by the discovery of aripiprazole (**1**); a D_2R partial agonist marketed for the treatment of schizophrenia. Although a number of D_2R partial agonists have entered clinical trials, aripiprazole remains the sole example of this ligand class in the clinic. More recently,

aripiprazole has been shown to display biased agonism, and it has been postulated that this bias may underlie its clinical efficacy.[10,11] As such, it is important to understand the SAR of biased ligands at the D_2R given a number of other D_2R partial agonists are also currently in clinical trials for the treatment of schizophrenia, including cariprazine (**2**).[12-14]

The 1,2,3,4-tetrahydroisoquinoline (THIQ) moiety has been explored as an isostere for the D_2-like receptor privileged phenylpiperazine scaffold.[15-17] Indeed exploration of this structure has yielded the D_3R subtype-selective antagonist SB269652 (**3**), although more recently this compound has been suggested to act as a negative allosteric modulator at the D_2R.[15,18] Our own exploration of this scaffold revealed *tert*-butyl (*trans*-4-(2-(3,4-dihydroisoquinolin-2(1*H*)-yl)ethyl)cyclohexyl)carbamate (**4**), a novel D_2R partial agonist with sub-micromolar potency and structural similarities to cariprazine (Figure 1). To further probe this finding, we generated derivatives focused on three main portions of the lead compound: the tertiary amine-containing "head group"; the cyclohexylene "spacer" group, and the *tert*-butyl carbamate "tail group" as seen in Figure 2. We combined this approach with novel analytical pharmacology methods[19] that allow us to quantify biased agonism and gain novel insight around SAR for the fine control of ligand efficacy and biased signaling at the D_2R.

Results

Chemical Synthesis

The synthesis of all compounds followed the procedures outlined in Schemes 1-7. Ethyl 2-(*trans*-4-aminocyclohexyl)acetate (**8**) was synthesized by hydrogenation of 4-nitrophenylacetic acid (**5**) in a Parr shaker for 3 days at 60 psi, followed by ethyl ester formation in the presence of concentrated hydrochloric acid and ethanol. The *trans* stereoisomer (**8**) was isolated as the hydrochloride salt by fractional crystallization from diethyl ether and acetonitrile. This was then protected as the *tert*-butyl carbamate (**12**) with

di-*tert*-butyl dicarbonate in good yield. Other commercially available *trans* amino acids, notably *trans*-4-aminocyclohexanecarboxylic acid (**6**) and tranexamic acid (**7**), were transformed to their respective ethyl esters (**9** and **10**) as in the synthesis of **8**, then protected as the *tert*-butyl carbamate (**13** and **14**, respectively). For the synthesis of the *cis* stereoisomer, 2-(*cis*-4-((*tert*-butoxycarbonyl)amino)cyclohexyl)acetic acid (**11**) was commercially supplied, and prepared as the ethyl ester (**15**) following Steglich esterification conditions using EDCI, shown in Scheme 1. This was applied to prevent deprotection of the *tert*-butyl carbamate group under general Fischer esterification conditions. The prepared ethyl ester materials (**12-15**) were then reduced to their respective aldehydes (**16-19**) using DIBALH, generally in near-quantitative yields.

The aromatic spacer was prepared according to Scheme 2. 4-Nitrophenylacetic acid (**5**) was initially converted to the ethyl ester using Fischer esterification conditions, then reduced to the corresponding aniline (**20**) in the presence of tin and concentrated hydrochloric acid. Following basic workup, **20** was protected as the *tert*-butyl carbamate (**21**), then treated with DIBALH to furnish the target aldehyde (**22**) in good overall yield. The head groups were either commercially supplied (**23**, **27**, **28**) or synthetically prepared as described in Scheme 3. Nitration of **23** in concentrated sulfuric acid with slow addition of sodium nitrate afforded **24** in good yield. The preparation of 1-(2,3-dichlorophenyl)homopiperazine (2,3-DCPHP, **26**) followed a literature procedure by Allen et al.[11] Buchwald-Hartwig amination of 1-bromo-2,3-dichlorobenzene (**25**) with homopiperazine in the presence of BINAP, tris(dibenzylideneacetone)dipalladium(0), potassium *tert*-butoxide and di-*tert*-butyl dicarbonate afforded the protected product, which was deprotected in situ (**26**), in low overall yield (3%).

Scheme 4 describes the synthesis of target compounds with variations to the head groups (**4**, **29-32**) through reductive alkylation of **16** with a respective amine (**23**, **24**, **26-28**) in 1,2-

DCE with sodium triacetoxyborohydride, generally in moderate yields following purification. The synthesis of THIQ-containing target compounds with variations to the tail group (**35-42**), shown in Scheme 5, required deprotection of the *tert*-butyl carbamate derivatives (**4**, **30**) by trifluoroacetic acid, followed by basic work-up to give the free amines (**33** and **34**) generally in high yields. Treatment of the amine with acetic anhydride in the presence of Hünig's base furnished the corresponding acetamide derivatives (**35** and **36**) in good yields. A range of carbamates (**37-40**) was synthesized in good yields using the corresponding chloroformates (isopropyl, isobutyl or phenyl chloroformate) or diethylpyrocarbonate. The synthesis of the urea-containing tail group was achieved with either dimethylcarbamyl chloride to give the *N*,*N*-dimethylurea (**41**) in good yield, or 1,1'-carbonyldiimidazole-mediated coupling with *tert*-butylamine to furnish the *tert*-butyl urea derivative (**42**) in moderate yield. These modifications afforded a range of target compounds with variations to the tail group.

The synthesis of compounds with variations in length and nature of the spacer group (**43-49**), illustrated in Scheme 6, followed reductive alkylation conditions with a respective aldehyde (**17-19**, **22**) in 1,2-DCE with sodium triacetoxyborohydride, generally in moderate yields following purification. This afforded a range of compounds containing the THIQ (**43-46**), or 2,3-DCPP (**47-49**) head groups with various spacers. Finally, the synthesis of compounds with the *N*,*N*-dimethylurea tail group (**2**, **54-56**), depicted in Scheme 7, followed the same general procedure as outlined in Scheme 5 for the synthesis of compounds with variations to the tail group.

Analytical approach to quantifying stimulus bias from concentration-response curves

To confirm on-target activity, all compounds were tested for their ability to displace the radiolabeled antagonist [^{3}H]spiperone at the human $D_{2L}R$ expressed in FlpIn CHO cell membranes (**Tables 1-4; Supplementary Tables 1 and 2**). In addition, to assess their functional activity, all compounds were tested for their ability to stimulate D_2R mediated inhibition of forskolin-stimulated cAMP production. This endpoint represents a canonical $D_{2L}R$ signaling pathway mediated by coupling to $G_{i/o}$ proteins that, in turn, inhibit adenylate cyclase. We then explored whether such molecular determinants were also important for another $D_{2L}R$ mediated pathway. Compounds were tested in an assay measuring phosphorylation of ERK1/2 through activation of the $D_{2L}R$ expressed in FlpIn CHO cells. The potency (pEC_{50}) and maximal responses (E_{max} as a percentage relative to the maximal effect of dopamine) of the various compounds are displayed in Supplementary Tables 1 and 2. Although reversals in orders of potency or maximal effect are indicators of biased agonism, the comparison of rank orders of potency or efficacy represents a sub-optimal approach to identify biased agonists.[20] Using potency values to characterize and quantify agonist activity is inadequate for agonists that produce different maximal responses and using maximal responses alone fails to differentiate between full agonists.[4] Therefore, a methodology that captures information encoded by the entire concentration-response relationship and relates this to changes in ligand structure will be far more likely to develop useful SAR around a biased ligand. We have developed an analytical approach that satisfies these criteria based on the 'Operational Model of Agonism' first derived by Black and Leff.[21] Using this approach we can obtain the functional equilibrium dissociation constant, i.e. affinity, for the receptor (denoted as K_A) coupled to a particular effector protein of signaling pathway, and τ, which encompasses both the intrinsic efficacy of the agonist in activating a particular cellular response pathway and receptor density. The values can be combined to give a "transduction coefficient" (τ/K_A), as an overall measure of the power of an agonist.

Values of log(τ/K_A) can be normalized to the reference agonist, dopamine, to cancel the impact of post-receptor "system bias" (which would be common to all ligands), yielding values of Δlog(τ/K_A). These values can then be compared across pathways for each ligand to give values of $\Delta\Delta$log(τ/K_A), a quantitative measure of bias between two different pathways.[6] Using this methodology we can relate changes in chemical structure to changes in functional affinity (K_A), efficacy (τ) or bias ($\Delta\Delta$log(τ/K_A)) between two signaling pathways.

Pharmacological Profiling of Compounds

The lead compound (**4**) acted as a partial agonist in both the cAMP assay and the pERK1/2 assay with sub-micromolar affinity (K_i = 741 nM) for the $D_{2L}R$ as determined by ligand binding (**Table 1**). Compound **4** did not show significant bias towards one signaling pathway as compared to dopamine ($\Delta\Delta$log(τ/K_A) = 0.51 ± 0.23). Subtle minimization of tail group branching to give the isopropyl carbamate (**38**) resulted in no change in affinity relative to **4**, and a loss of detectable agonism in the pERK1/2 assay. In the cAMP assay a significant 4-fold decrease in efficacy (τ) was observed (**Table 1**). Further minimization of branching to the ethyl carbamate (**37**) caused no significant change in affinity relative to **4**, and again no agonism in the pERK1/2 assay. However, in the cAMP assay, a 6-fold increase in functional affinity (pK_A) was accompanied by a 5-fold decrease in efficacy (τ). This results in a similar transduction coefficient for **4** and **37** in the cAMP assay. However, subtle modification to the isobutyl carbamate (**39**) significantly reduced the transduction coefficient relative to **4** in the cAMP assay and resulted in a complete loss of efficacy in the pERK1/2 assay. Similarly, incorporation of aromaticity to the tail group with the phenyl carbamate (**40**) resulted in a significant 20-fold decrease in the transduction coefficient in the cAMP assay as compared to **4** and no detectable agonism in the pERK1/2 assay. Modification of the tail group of **4** to the acetamide (**35**) resulted in complete loss of agonism in the pERK1/2 assay and a significant

decrease in efficacy (τ) in the cAMP assay. Modification of the tail group from *tert*-butyl carbamate to *tert*-butyl urea (**42**) showed similar affinity to **4** in a radioligand binding assay, no agonist activity in the pERK1/2 assay and a significant 6-fold decrease in efficacy (τ) in the cAMP assay. As such, all of the above modifications to the tail group of **4** abrogated detectable agonism in the pERK1/2 assay, and either maintained or reduced agonist efficacy in the cAMP assay. Modification to the *N*,*N*-dimethylurea (**41**) which represents the tail group of cariprazine (**2**), caused no significant change in functional affinity or efficacy in the cAMP assay, indicating that **41** has equivalent activity to **4** in this functional endpoint (**Figure 3**). As this compound showed no agonist activity in the pERK1/2 assay, and is therefore less active than **4** at this functional endpoint, this modification confers bias towards the cAMP pathway.

We next focused on the role of the spacer group of **4** (**Table 2**). Modification from the *trans* to the *cis* stereoisomer (**45**) resulted in a similar binding affinity relative to **4**, but a complete loss of agonist efficacy in the pERK1/2 assay. Furthermore, in the cAMP assay this modification resulted in a significant 8-fold increase in functional affinity (pK_A) but no change in efficacy (τ). Overall this resulted in a significant increase in the transduction coefficient in the cAMP assay. Given that **45** was inactive in the pERK1/2 assay, this clearly demonstrates that this modification caused an increase in bias towards the cAMP pathway (**Figure 4**). This effect was not observed with corresponding compounds in which the *tert*-butyl carbamate tail group was replaced with *N*,*N*-dimethylurea. Indeed, with the *N*,*N*-dimethylurea tail group, modification from *trans* (**41**) to *cis* stereoisomer (**54**) resulted in no significant change in all parameters relating to the cAMP assay (Student's t-test, $p > 0.05$) and **54** maintained no agonist efficacy in the pERK1/2 assay, although a significant loss of binding affinity (pK_i) was observed as compared to **41**. We then explored further subtle modifications to the spacer group of **4**. Truncation of the spacer group by 1 carbon (**43**)

caused no significant change in overall bias as compared to **4**. However, rather than the transduction coefficients remaining unchanged at both pathways, a significant 5-fold increase in the transduction coefficient at the cAMP assay was cancelled out by a significant 5-fold increase in efficacy (τ) observed in the pERK1/2 assay. Shifting the spacer group one carbon towards the THIQ head group (**44**) had no significant effect upon binding affinity (p*K*i) as compared to **4**. In the pERK1/2 assay, this compound behaved as a very weak partial agonist. Consequently estimates of functional affinity in this assay were associated with significant error and, as such, changes in bias as compared to **4** were not statistically significant. Finally, incorporation of aromaticity to the spacer group (**46**) resulted in similar binding affinity as **4**, but with a significant decrease of transduction coefficient in the cAMP assay, and no detectable response in the pERK1/2 assay.

Next we explored modification of the THIQ head group (**Table 3** and **4**). Stemp et al. demonstrated that deactivation of the THIQ ring through 6- or 7-subtitutions has little impact on activity at D_2-like receptors,[15] and we sought to explore this effect with a focus on agonist efficacy at the $D_{2L}R$. Due to synthetic accessibility and commercial availability, we explored THIQ deactivating groups in the 7-position. Incorporation of the 7-nitro substituent (**29**) resulted in a loss of agonism in both assays, with no change in binding affinity. Modification to the nitrile substituent (**30**), which shares structural similarities with SB269652 (**3**), resulted in a loss of agonist efficacy in the pERK1/2 assay, and a significant 4-fold decrease in efficacy in the cAMP assay, with no significant change in binding affinity. Of interest, the 7-cyano derivative with the acetamide tail group (**36**) displayed a significant 32-fold higher binding affinity than **4**, albeit with loss of agonism at both signaling endpoints measured. Furthermore, direct comparison with **35** (**Table 1**) reveals that the addition of a cyano group at position 7 confers a 260-fold increase in the affinity determined by radioligand binding.

These results infer that THIQ ring deactivation can have significant effects on binding affinity, but consistently have a detrimental effect upon agonism.

Mindful of the structural similarities of **4** to cariprazine (**2**), we next explored modification of the THIQ head group to 2,3-DCPP (**Table 4**). As a general observation, this modification resulted in higher binding affinity than equivalent compounds with the THIQ head group (**Tables 1-4**). Direct replacement of the THIQ moiety of **4** for 2,3-DCPP (**32**) resulted in a significantly (19-fold) increased affinity at the $D_{2L}R$ as determined by radioligand binding (Student's t-test $P < 0.05$). In contrast, values of τ or pK_A determined in both pERK1/2 and cAMP assays did not differ significantly from that of **4** (Student's t-test $P > 0.05$). Introduction of the *N*,*N*-dimethylurea tail group (cariprazine, **2**) did not change binding affinity relative to **32** (**Table 4**). However, while pK_A or τ did not change significantly in the pERK1/2 assay, a significant 30-fold increase in functional affinity ($pK_A = 8.71$) was observed in the cAMP assay relative to that of **32** (**Figure 5**). This conferred a large increase in bias towards the cAMP pathway relative to **32**, **4** and dopamine (42-fold, 68-fold and 218-fold respectively). Of interest, a similar pattern was observed in the corresponding compounds containing the THIQ core (**4** vs **41**, **Figure 3**) although in this case, a lack of detectable agonism in the pERK1/2 assay for **41** meant that the degree of bias conferred by this modification could not be quantified.

We then focused on the role of the spacer group with 2,3-DCPP head group in place. Modification of the spacer configuration from *trans* (**32**) to *cis* stereoisomer (**49**) resulted in similar binding affinity to **32**, as was observed for the corresponding compounds in the THIQ series (*trans*; **4**, *cis*; **45**). However, unlike the increase in bias observed for **45** as compared to **4**, no change in bias was observed for **49** relative to **32**. Modification of cariprazine (**2**) to the *cis* stereoisomer (**56**) caused a loss of agonism in the pERK1/2 assay. However this was also accompanied by both a significant (50-fold) decrease in functional affinity (pK_A) and a

significant 8-fold decrease in efficacy (τ) in the cAMP assay relative to cariprazine (**2**) (Student's t-test, $P < 0.05$). As such, it is not clear whether this chemical modification influences bias. Further subtle modifications to the spacer group of **32** were then investigated. Truncation of the spacer group of **32** by one carbon (**47**) caused a significant 8-fold decrease in affinity measured by radioligand binding. However, this modification caused markedly different effects upon efficacy and functional affinity in the two different assays. In the pERK1/2 assay a significant 120-fold decrease in functional affinity (pK_A) was accompanied by a significant 10-fold increase in τ. In the cAMP assay no significant change in either parameter was observed. Consequently this modification confers 6-fold bias towards the cAMP pathway relative to **32**. Shifting the spacer group of **32** by 1 carbon towards the 2,3-DCPP head group (**48**) caused no significant change in bias, although this modification did cause a significant 9-fold loss of affinity (pK_i). In contrast, shifting the spacer group of cariprazine (**2**) towards the 2,3-DCPP head group (**55**) caused a significant 84-fold decrease in bias towards the cAMP pathway (Student's t-test, $p > 0.05$) and as such a bias profile not significantly different to that of **32**. This effect was predominantly mediated by a significant 61-fold decrease in functional affinity (pK_A) in the cAMP assay (Student's t-test, $p < 0.05$). However significant 3-fold and 4-fold decreases in intrinsic efficacy (τ) were observed in the pERK1/2 and cAMP assays respectively (Student's t-test, $p < 0.05$). Ring expansion to 2,3-DCPHP (**31**) yielded the compound with the highest binding affinity of the series but with loss of efficacy in both assays.

Compound **4** and cariprazine (**2**) display significantly different (60-fold) bias profiles between an assay measuring cAMP, and that measuring phosphorylation of ERK1/2, with cariprazine demonstrating 230-fold bias towards the cAMP pathway as compared to dopamine. Although both compounds have a conserved spacer group they differ in their head group (**4**; THIQ, **2**; 2,3-DCPP) and in their tail group (**4**; *tert*-butyl carbamate, **2**; *N*,*N*-

dimethylurea). Exchange of the *tert*-butyl carbamate for *N*,*N*-dimethylurea conferred bias towards the cAMP pathway to the THIQ derivative (**41**). The opposite modification decreased bias of the 2,3-DCPP derivative (**32**). This observation is consistent with *N*,*N*-dimethylurea substitution of the tail group conferring bias towards cAMP. This raises the possibility that the tail group extends in to, and interacts with a secondary (or allosteric) pocket. Indeed, a dualsteric or bitopic (orthosteric/allosteric) mode of interaction has been suggested to underlie the biased actions of a number of GPCR ligands.[22,23] However, this pattern becomes more complex as we consider further derivatives of these ligands whereby conserved structural modifications have a differential impact upon biased agonism depending upon the head group. Focusing upon compounds with the *tert*-butyl carbamate head group, a comparison of *trans* (**4**; THIQ, **32**; 2,3-DCPP) with the corresponding *cis* stereoisomer revealed that this modification confers bias towards the cAMP pathway for the compound containing the THIQ head group (**45**) but not for the compound containing the 2,3-DCPP head group (**49**). Conversely truncation of the spacer region of **4** and **32** by one carbon atom confers bias towards the cAMP pathway for the compound containing the 2,3-DCPP head group (**47**) but not for the corresponding compound with a THIQ head group (**43**). Furthermore, comparison of **43** and **47** revealed that exchange of the THIQ head group for the 2,3-DCPP head group conferred bias towards cAMP underpinned by a large decrease in functional affinity in the pERK1/2 assay (**Figure 6**). This is distinct from the lack of bias observed between **4** and **32**, which differ only by an additional carbon within the spacer group. This then suggests that the nature and relative orientation of both the head and tail group can impact the bias profile of this series of compounds. It should be noted that the structural changes that can engender significant changes in bias within this study are often relatively subtle. Such an observation is not surprising if one considers the relatively modest changes in the orthosteric binding site of active agonist bound receptor crystal structures, for

example those of the β_2-adrenoceptor, when compared to the corresponding antagonist bound structures.[24-27] Such minor movements are coupled to major structural movements at the cytosolic face of the receptor, allowing signalling proteins such as G proteins to bind. Indeed, the structural difference between GPCR agonists and antagonists can also be subtle.[28] Accordingly, we can expect that structural changes that determine differential agonist action at one pathway as compared to another will also be subtle. As such the SAR around bias represents a challenge, but the use of the operational model to identify and quantify changes in bias profile and relate them to such subtle changes is a valuable approach to meet this challenge.

In view of the therapeutic importance of the D_2R, it is not surprising that a number of studies have explored the molecular determinants of efficacy at this receptor.[11,29-34] Notably, Allen et al. applied a combinatorial approach to explore the SAR around aripiprazole (**1**), and identified β arrestin-biased agonists based on a similar scaffold.[11] Another study investigated determinants of efficacy (for activation of $G\alpha_{i/o}$ proteins) at the D_3R for a series of compounds containing the phenylpiperazine moiety.[35] Newman et al. demonstrated a progressive decrease in efficacy of such compounds with the incremental addition of methylene units to the phenylpiperazine moiety in a series of 2,3-DCPP derivatives. In contrast similar modifications to a series of 2-methoxyphenylpiperazine derivatives were weak partial agonists. Using molecular docking and modeling approaches, the authors suggested that as the linker length increased in the 2,3-DCPP series, the orientation of the 2,3-DCPP moiety became similar to that in the 2-methoxyphenylpiperazine series and could no longer form hydrogen bonding interactions with the conserved serines within TM5.

We performed molecular docking experiments to gain insight into the binding mode of such biased agonists at the D_2R. Following molecular dynamics simulations over 200 ps, we

compared the final binding mode of **32** and **2** (**Figure 7A**); compounds that displayed 60-fold differentiation in their bias profiles yet differ only in the nature of the tail group. The predicted binding modes illustrate that while the tail group and spacer regions adopt a similar position, the 2,3-DCPP moiety adopts a divergent pose (**Figure 7B**). This in turn results in distinct differences in receptor structure between the two models with noticeable variation in the orientations of conserved serines in TM5 (Ser5.42, Ser5.43 & Ser5.46), Phe5.47 and Tyr7.35. In particular, a H-bond interaction between Ser5.46 and Tyr3.37 in the ligand-receptor complex of **32** is absent in the corresponding ligand-receptor complex of **2** (**Figure 7A**). It should be noted that neither compound forms H-bond interactions with the TM5 serines in agreement with the study by Newman et al.[35] Comparison of *trans* and *cis* stereoisomers with the THIQ head group (**4** and **45**), respectively, in equivalent dynamics simulations revealed significant divergence in both the orientation of the head and tail groups (**Figure 7C & D**). These isomers display distinct bias profiles, and it is interesting to note the distinct orientation of residues within TM5 and TM6 between the two complexes. In particular, we again observe a large movement of Phe5.47, a large movement of Phe6.51 and, notably, the different position of Trp6.48 between the two complexes. With both examples, it appears that subtle structural differences within the tail group or spacer region cause distinct changes in the position of the head group within the orthosteric pocket and a concomitant change of conformation within this binding pocket. This in turn underlies the bias profiles of such compounds. Although such modeling and docking experiments are intrinsically associated with a degree of speculation it is interesting to note that these results are consistent with those of Newman et al.[35] A study by Tschammer et al. also focused on 1,4 disubstituted phenylpiperazine derivatives at the D_2R.[32] Within this study it was observed that rigidly constraining the methoxy group of the 2-methoxyphenylpiperazine head group through derivatization to the sterically demanding (2,3-dihydrobenzofuran-7-yl)piperazine abolished

the activity of this compound in a cAMP assay whilst maintaining partial agonist activity in a pERK1/2 assay.[32] Such a finding is consistent with bias being driven through different orientations of the head group within the orthosteric pocket.

To our knowledge this is the first study to apply a quantitative pharmacological approach using the operational model of agonism to enrich a comprehensive SAR study focused upon biased agonism at the D_2R. A number of methods to quantify bias have been proposed and published in recent times[6] with particular attention given to the relative merits of the transduction ratio method used in this study, as compared to the sigma method proposed by Rajagopal et al.[20] Although both methods use the operational model of agonism the latter fixes the values of functional affinity (K_A) to that determined by radioligand binding (K_i), whereas the method used in our study derives the K_A directly from the fitting of the dose-response curves to the operational model of agonism. Thus this operationally derived K_A represents the functional affinity of an agonist associated with that particular signaling pathway. Of note, the affinity determined in our radioligand binding experiments is significantly different to that determined in one or both of our functional assays 11 out of 26 times (42%) (**Tables 1**, **2** and **4**). In 8 cases this difference is greater than 10-fold, and for **54**, a difference of more than 100-fold is observed. Furthermore, there is no pattern to the distribution of the values of pK_A that differ significantly from the corresponding value of pK_i, with examples in both functional assays. Indeed, we obtained values of pK_A both smaller and greater than the corresponding pK_i value. As such fixing the K_A to that determined in a radioligand-binding assay would introduce significant error into estimates of transduction coefficients, and ultimately identification of ligand bias. Furthermore, it should be noted that the pK_i determined for a ligand in a radioligand binding assay can depend on the radiolabelled probe (agonist versus antagonist) used or the experimental design (components

of buffer, whole cells versus membranes, the presence of guanine nucleotide). Taking dopamine as an example, a study performed using CHO cell membranes expressing the $D_{2L}R$ determined a pK_{i_high} of 58 nM, a pK_{i_low} of 3420 nM and a pK_i determined using the agonist [^{3}H]NPA as the radioligand as 8 nM.[36] This begs the question, if one were to fix the value of pK_A to a value of pK_i determined by binding affinity, which would be most appropriate? We observed no pattern in the way in which the functional affinities determined for the agonists within this series deviated from the corresponding pK_i values. Thus we conclude that no value of affinity determined in a binding assay will be a good predictor of functional affinity. Although significant differences in τ were observed across the chemical series, it is interesting to note that in all cases in which a chemical modification engenders a significant change in bias, this change is predominantly driven by a change in functional affinity for one assay (change in pK_{A_cAMP} **32** vs **2**, 40-fold; **55** vs **2**, 60-fold: change in $pK_{A\_pERK1/2}$: **43** vs **47**; 112-fold; **32** vs **47**, 120-fold). This is perhaps not surprising given that **4**, cariprazine (**2**), and derivatives thereof, behave as partial agonists and thus have relatively small values of τ. Thus changes in τ will have a much smaller impact upon the overall transduction coefficient ($\log(\tau/K_A)$) as compared to changes in functional affinity for low efficacy agonists. Apart from the identification and quantification of biased agonism, another key challenge is relating the bias profile of a ligand to a physiological response in vivo. As such, the identification of pairs of ligands that are structurally similar and have similar binding affinity for the receptor target, yet display distinct bias profiles (such as compounds **2** and **32**), may prove to be useful tools to investigate the therapeutic relevance of biased agonism.

Conclusion

Biased agonism represents an attractive paradigm that can be exploited in the design of novel selective GPCR ligands. However, the identification and quantification of bias remains a

challenge. In this study, we have addressed this challenge by applying detailed pharmacological profiling to a series of compounds based on the hit compound *tert*-butyl (*trans*-4-(2-(3,4-dihydroisoquinolin-2(1*H*)-yl)ethyl)cyclohexyl)carbamate (**4**), a $D_{2L}R$ partial agonist with structural similarity to cariprazine (**2**). We combined this approach with analytical methods to allow us to identify and quantify biased agonism. We demonstrated that **4** displayed no significant bias between the two signaling endpoints; ERK1/2 phosphorylation and inhibition of forskolin-stimulated cAMP production, as compared to dopamine. In contrast, cariprazine (**2**), awaiting FDA approval for the treatment of schizophrenia, displayed greater than 200-fold bias towards the cAMP pathway. Taking advantage of these distinct bias profiles, we explored the SAR of biased agonism around these two compounds. We discovered that the nature of the head group, composition of the tail group, orientation, length and flexibility of the spacer are all important factors for the control of biased agonism at the $D_{2L}R$. Our molecular modeling studies suggest that subtle changes in the spacer and tail region can influence the orientation of the head group within the orthosteric pocket and these distinct orientations may underlie patterns of biased agonism. Using the transduction coefficient method, we demonstrated that the functional affinities of such ligands can differ significantly from those determined in radioligand binding, and that instances of significant changes in bias were driven largely by changes in the functional affinity of a ligand at a particular pathway. In conclusion, this approach has provided an unprecedented insight into the molecular determinants and SAR of biased agonism at the $D_{2L}R$. Given the clinical relevance of biased agonism at the $D_{2L}R$, this study may serve as the precursor to the development of novel biased ligands for this therapeutically important target.

Experimental

General Experimental

All reagents were purchased from Sigma-Aldrich, Alfa Aesar, AK Scientific or ChemImpex, and used without purification. GR grade ammonium hydroxide solution (28% aqueous solution), and LR grade methanol, ethyl acetate, chloroform, DCM and acetonitrile were purchased from Merck and used without further purification. All ^{1}H NMR and ^{13}C NMR spectra (DEPTQ) were recorded on a Bruker Avance III 400 Ultrashield Plus spectrometer at 400.13 and 100.62 MHz respectively. Results were recorded as follows: chemical shift values are expressed as δ units generally acquired in $CDCl_3$; or CD_3OD, D_2O or d_6-DMSO where specified, with tetramethylsilane (0.00 ppm) as reference for ^{1}H NMR (residual solvent peak as reference for ^{13}C NMR),[37] multiplicity (singlet (s), doublet (d), triplet (t), quartet (q), broad (br), multiplet (m), doublet of doublets (dd), doublet of triplets (dt), triplet of triplets (tt), quartet of doublets (qd)), coupling constants (*J*) in Hertz and integration. Thin-layer chromatography was conducted on 0.2 mm plates using Merck silica gel 60 F_{254}. Flash Chromatography was performed using Merck Silica Gel 60, 230-400 mesh ASTM. High resolution mass spectra (HRMS) were obtained on a Waters LCT Premier XE (TOF) using electrospray ionization (ESI) at a cone voltage of 50 V. LCMS data was obtained on an Agilent 1200 series LC coupled directly to a photodiode array detector and an Agilent 6100 Quadrupole MS, using a Phenomenex® column (Luna 5 µm C8, 50 mm × 4.60 mm ID). Analytical reverse-phase HPLC was performed on a Waters HPLC system coupled directly to a photodiode array detector and fitted with a Phenomenex® Luna C8 (2) 100 Å column (150 mm × 4.6 mm, 5 µm) using a binary solvent system; solvent A: 0.1% TFA/H_2O; solvent B: 0.1% TFA/80% CH_3CN/H_2O. Gradient elution was achieved using 100% solvent A to 100% solvent B over 20 min at a flow rate of 1 mL/min. All compounds were >95 % purity by HPLC (λ = 254, 214 nm) prior to biological testing. Melting point analysis was performed in duplicate on a Mettler Toledo MP50 Melting Point System.

*Ethyl 2-(*trans-*4-aminocyclohexyl)acetate hydrochloride* (**8**).[38] Following an adapted literature procedure,[38] 10% Pd/C (881 mg, 828 μmol) was carefully added to an orange suspension of **5** (5.00 g, 27.6 mmol) in H_2O (150 mL). The reaction mixture was hydrogenated on a Parr shaker at 60 psi at RT for 3 d, until the uptake of hydrogen was complete, and no starting materials remained by TLC ($CHCl_3/CH_3OH$, 1:1). The mixture was filtered through a Celite™ pad, washed with water (30 mL), and the filtrate evaporated to dryness *in vacuo* to reveal a white solid. The material was taken up in absolute EtOH (70 mL) to which concentrated HCl (10 mL) was added and the mixture heated at reflux for 2 h. TLC confirmed ethyl ester formation and the solvents were concentrated *in vacuo*. The material was basified with 1 M NaOH solution to pH 14, and a white precipitate emerged. The product was then extracted from the mixture with EtOAc (3 × 30 mL), and the combined organic extracts washed with brine, then dried over anhydrous Na_2SO_4. The product was then converted to the HCl salt by the addition of 1 M HCl in Et_2O (27.6 mL, 27.6 mmol), and the solvents concentrated to half volume *in vacuo*. The solution was then cooled to 0 °C, which resulted in fractional crystallisation of the *trans* stereoisomer as a white solid which was then collected by filtration and washed with cold CH_3CN (1.34 g, 22%). mp: 164–166 °C (lit.[39] 162–163 °C). ^{1}H NMR (MeOD) δ 4.11 (q, 2H, J = 7.1 Hz), 3.05 (tt, 1H, J = 11.8, 3.9 Hz), 2.24 (d, 2H, J = 7.0 Hz), 2.11 – 2.00 (m, 2H), 1.93 – 1.83 (m, 2H), 1.83 – 1.68 (m, 1H), 1.43 (qd, 2H, J = 12.8, 3.6 Hz), 1.24 (t, 3H, J = 7.1 Hz), 1.14 (qd, 2H, J = 13.3, 3.3 Hz). ^{13}C NMR (CD_3OD) δ 174.2 (C), 61.4 (CH_2), 51.2 (CH), 41.8 (CH_2), 34.7 (CH), 31.50 (CH_2), 31.47 (CH_2), 14.6 (CH_3).

trans-*Ethyl 4-aminocyclohexanecarboxylate* (**9**).[40] *trans*-4-Aminocyclohexanecarboxylic acid hydrochloride (**6**, 250 mg, 1.39 mmol) was taken up in absolute EtOH (10 mL) and concentrated HCl (2 mL), and the pale orange solution was heated at reflux for 3 d. The solution was concentrated in vacuo, diluted with water (10 mL), and made alkaline with

NH_4OH solution to pH 10. The product was extracted with EtOAc (2 × 30 mL) and the combined organic extracts washed with brine (15 mL), dried over anhydrous Na_2SO_4 and evaporated to dryness to give the product as a pale orange oil which required no further purification (194 mg, 81%). ^{1}H NMR δ 4.11 (q, *J* = 7.1 Hz, 2H), 2.66 (tt, *J* = 11.0, 3.9 Hz, 1H), 2.21 (tt, *J* = 12.3, 3.6 Hz, 1H), 2.03–1.85 (m, 4H), 1.56–1.39 (m, 4H), 1.25 (t, *J* = 7.1 Hz, 3H), 1.11 (qd, *J* = 13.0, 3.2 Hz, 2H). ^{13}C NMR δ 176.0 (C), 60.3 (CH_2), 50.0 (CH), 42.8 (CH), 35.8 (CH_2), 28.1 (CH_2), 14.3 (CH_3).

trans-*Ethyl 4-(aminomethyl)cyclohexanecarboxylate* (**10**).[41] Tranexamic acid (**7**, 1.00 g, 6.36 mmol) was taken up in absolute EtOH (30 mL) and concentrated HCl (5 mL). The colourless solution was heated at reflux for 2 h. The solution was then cooled to 0 °C on ice, then basified with 1 M NaOH solution (30 mL) to pH 12. The product was extracted with EtOAc (3 × 20 mL), the combined organic extracts washed with brine (20 mL), dried over anhydrous Na_2SO_4 and evaporated to dryness to reveal the product as a colourless oil which solidified on drying (775 mg, 66%). ^{1}H NMR δ 4.11 (q, *J* = 7.1 Hz, 2H), 3.32 (s, 2H), 2.61 (d, *J* = 6.5 Hz, 2H), 2.22 (tt, *J* = 12.2, 3.4 Hz, 1H), 2.07–1.95 (m, 2H), 1.95–1.82 (m, 2H), 1.51–1.33 (m, 3H), 1.25 (t, *J* = 7.1 Hz, 3H), 0.97 (qd, *J* = 13.0, 3.1 Hz, 2H). ^{13}C NMR δ 176.0 (C), 60.2 (CH_2), 47.9 (CH_2), 43.5 (CH), 39.4 (CH), 29.8 (CH_2) 28.6 (CH_2), 14.3 (CH_3).

General Procedure A (*tert*-Butyl Carbamate Protection of Primary Amine)

The amine (occasionally as the HCl salt, 1–1.2 equiv) was taken up in DCM (15–30 mL), and Et_3N (1.2 equiv, or 2.4 equiv if using hydrochloride salt) added. To the stirred solution at RT was added a solution of di-*tert*-butyl dicarbonate (1 equiv) in DCM (5 mL). The solution was stirred for 2–24 h, then diluted with DCM (20 mL), washed with 1 M $KHSO_4$ (2 × 20 mL), and brine (10 mL). The organic layer was dried over anhydrous Na_2SO_4 and evaporated to dryness *in vacuo* to reveal the title compound, which was purified by flash column chromatography if required.

*Ethyl 2-(*trans-*4-((tert-butoxycarbonyl)amino)cyclohexyl)acetate* (**12**).[42] Using **8** (682 mg, 3.07 mmol) as the starting material, following General Procedure A, gave the product as white needles (746 mg, 94%). Determination of diastereomeric purity (> 95% *trans*) was achieved by ^{1}H-NMR analysis. The *trans* stereoisomer (**12**) exhibited a characteristic resonance at δ 2.18 ppm, whilst the *cis* stereoisomer (**15**) exhibited the equivalent resonance at δ 2.24 ppm. ^{1}H NMR δ 4.52 (br s, 1H), 4.12 (q, *J* = 7.1 Hz, 2H), 3.37 (br s, 1H), 2.18 (d, *J* = 6.9 Hz, 2H), 2.04–1.95 (m, 2H), 1.84–1.66 (m, 3H), 1.43 (s, 9H), 1.25 (t, *J* = 7.1 Hz, 3H), 1.20–1.01 (m, 4H). ^{13}C NMR δ 172.8 (C), 155.2 (C), 78.9 (C), 60.1 (CH_2), 49.4 (CH), 41.4 (CH_2), 33.4 (CH), 33.1 (CH_2), 31.5 (CH_2), 28.4 (CH_3), 14.2 (CH_3).

trans-*Ethyl 4-((tert-butoxycarbonyl)amino)cyclohexanecarboxylate* (**13**).[43] Using **9** (190 mg, 1.11 mmol) as the starting material, following General Procedure A. The product was purified by flash column chromatography (Petroleum spirits/EtOAc, 10:1) to give the title compound as white needles (174 mg, 58%). ^{1}H NMR δ 4.40 (br s, 1H), 4.11 (q, *J* = 7.1 Hz, 2H), 3.41 (br s, 1H), 2.20 (tt, *J* = 12.1, 3.5 Hz, 1H), 2.12–1.93 (m, 4H), 1.52 (qd, *J* = 12.6, 3.2 Hz, 2H), 1.44 (s, 9H), 1.24 (t, *J* = 7.1 Hz, 3H), 1.11 (qd, *J* = 12.7, 3.3 Hz, 2H). ^{13}C NMR δ 175.6 (C), 155.3 (C), 79.4 (C), 60.4 (CH_2), 49.1 (CH), 42.6 (CH), 32.7 (CH_2), 28.5 (CH_3), 27.9 (CH_2), 14.3 (CH_3).

trans-*Ethyl 4-(((tert-butoxycarbonyl)amino)methyl)cyclohexanecarboxylate* (**14**). Using **10** (713 mg, 3.85 mmol) as the starting material, following General Procedure A, gave the title compound as a pale yellow oil (880 mg, 96%). ^{1}H NMR δ 4.63 (br s, 1H), 4.11 (q, *J* = 7.1 Hz, 2H), 2.98 (t, *J* = 6.4 Hz, 2H), 2.21 (tt, *J* = 12.2, 3.6 Hz, 1H), 2.06–1.92 (m, 2H), 1.89–1.74 (m, 2H), 1.50–1.33 (m, 12H), 1.24 (t, *J* = 7.1 Hz, 3H), 0.96 (qd, *J* = 13.1, 3.4 Hz, 2H). ^{13}C NMR δ 176.0 (C), 156.2 (C), 79.2 (C), 60.3 (CH_2), 46.7 (CH_2), 43.4 (CH), 37.9 (CH), 29.8 (CH_2), 28.6 (CH_2), 28.5 (CH_3), 14.3 (CH_3).

*Ethyl 2-(*cis*-4-((tert-butoxycarbonyl)amino)cyclohexyl)acetate* (**15**). To a solution of commercially available 2-(*cis*-4-((*tert*-butoxycarbonyl)amino)cyclohexyl)acetic acid (**11**, 500 mg, 1.94 mmol) in DCM (10 mL) at RT was added 1-ethyl-3-(3-dimethylaminopropyl)carbodiimide hydrochloride (410 mg, 2.14 mmol), followed by a 4-(dimethylamino)pyridine (5 mol%, 12 mg, 97.2 μmol). After 15 min, absolute EtOH (15 mL) was added, and the mixture stirred overnight. TLC confirmed reaction completion (petroleum spirits/EtOAc, 3:1) and the mixture was concentrated in vacuo, then taken up in EtOAc (30 mL) causing a precipitate to emerge. The mixture was then washed with 1 M $KHSO_4$ (2 × 20 mL), brine (20 mL), dried over anhydrous Na_2SO_4 and evaporated to dryness to reveal a colourless oil (354 mg, 64%) which required no further purification. ^{1}H NMR δ 4.65 (br s, 1H), 4.13 (q, J = 7.1 Hz, 2H), 3.72 (s, 1H), 2.24 (d, J = 7.3 Hz, 2H), 2.00–1.84 (m, 1H), 1.70–1.53 (m, 6H), 1.50–1.37 (m, 9H), 1.33–1.16 (m, 5H). ^{13}C NMR δ 172.8 (C), 155.2 (C), 79.0 (C), 60.2 (CH_2), 46.2 (CH), 40.4 (CH_2), 32.8 (CH), 29.5 (CH_2), 28.4 (CH_3), 27.6 (CH_2), 14.3 (CH_3).

General Procedure B (Reduction of Ester to Aldehyde)

The ethyl ester (1 equiv) was taken up in toluene (15-30 mL), degassed with nitrogen bubbling for 15 min, then cooled to -78 °C on a dry ice/acetone bath for a further 10 min. To the stirring colourless solution under nitrogen, was slowly added DIBALH (1 M in toluene, 2 equiv) dropwise over 15 min. The mixture stirred at -78 °C until foaming of the reaction mixture stopped (30–60 min). The mixture was then quenched with CH_3OH (10–20 mL) in toluene (10 mL), and warmed to RT with stirring for 15 min. Saturated potassium sodium tartrate solution (30 mL) was added and the mixture stirred vigorously for 30 min. The product was then extracted with Et_2O (3 × 30 mL), and the combined organic extracts dried over anhydrous Na_2SO_4 and evaporated to dryness to give the crude compound. If required, the product was purified by flash column chromatography.

tert-*Butyl (*trans-*4-(2-oxoethyl)cyclohexyl)carbamate* (**16**).[15] Using **12** (1.25 g, 4.38 mmol) as the starting material, following General Procedure B, the material was purified by column chromatography (petroleum spirits/EtOAc, gradient 6:1 to 4:1) gave the title compound as a white wax (944 mg, 89%, lit.[15] 53%). ^{1}H NMR δ 9.75 (t, *J* = 2.0 Hz, 1H), 4.47 (br s, 1H), 3.37 (br s, 1H), 2.32 (dd, *J* = 6.6, 2.0 Hz, 2H), 2.04–1.97 (m, 2H), 1.89–1.75 (m, 3H), 1.45 (s, 9H), 1.21–1.03 (m, 4H). ^{13}C NMR δ 202.2 (CH), 155.3 (C), 79.2 (C), 50.7 (CH_2), 49.5 (CH), 33.2 (CH_2), 31.8 (CH_2), 31.7 (CH), 28.5 (CH_3).

tert-*Butyl (*trans-*4-formylcyclohexyl)carbamate* (**17**).[44] Using **13** (160 mg, 590 μmol) as the starting material, following Procedure B, gave the title compound as a white wax (134 mg, 99%). ^{1}H NMR δ 9.62 (s, 1H), 4.44 (br s, 1H), 3.40 (br s, 1H), 2.21–1.97 (m, 5H), 1.51–1.27 (m, 11H), 1.22–1.10 (m, 2H). ^{13}C NMR δ 203.9 (CH), 155.5 (C), 81.6 (C), 49.4 (CH), 32.2 (CH_2), 28.5 (CH_3), 24.9 (CH_2), 19.5 (CH).

tert-*Butyl ((*trans-*4-formylcyclohexyl)methyl)carbamate* (**18**).[45] Using **14** (850 mg, 2.98 mmol) as the starting material, following Procedure B. The crude material was used immediately in subsequent reactions to avoid rapid degradation. To confirm aldehyde formation the crude material (150 mg) was taken up in absolute ethanol (15 mL), and was added a solution of 2,4-DNP (50 mg) in EtOH (5 mL) and concentrated H_2SO_4 (1 mL). The solution was heated at reflux for 1 h, then allowed to cool revealing a yellow precipitate. The product was collected by filtration and washed with ethanol to give (*trans*-4-((2-(2,4-dinitrophenyl)hydrazono)methyl)cyclohexyl)methanaminium sulfate as a yellow solid. Formation of the 2,4-DNP derivative was confirmed by LCMS. ESI-MS (*m*/*z*): 322.2 (MH^+).

*tert-Butyl (*cis-*4-(2-oxoethyl)cyclohexyl)carbamate* (**19**).[46] Using **15** (400 mg, 1.40 mmol) as the starting material, following Procedure B, gave the title compound as a pale yellow wax (325 mg, 96%). ^{1}H NMR δ 9.76 (t, *J* = 2.1 Hz, 1H), 4.63 (s, 1H), 3.78–3.64 (m, 1H), 2.37 (dd, *J* = 6.9, 2.1 Hz, 2H), 2.10–1.95 (m, 1H), 1.68–1.58 (m, 6H), 1.44 (s, 9H), 1.35–1.19 (m,

2H). ^{13}C NMR δ 202.3 (CH), 155.7 (C), 79.3 (C), 49.7 (CH_2), 46.3 (CH), 30.6 (CH), 29.6 (CH_2), 28.6 (CH_3), 28.0 (CH_2).

Ethyl 2-(4-aminophenyl)acetate (**20**).[47] 4-Nitrophenylacetic acid (**5**, 1.00 g, 5.52 mmol) was taken up in EtOH (20 mL) and concentrated HCl (2 mL). The solution was stirred at reflux for 2 h. The mixture was left open to evaporate slowly over 3 d causing crystallisation of the product, which was filtered and washed with 5% NH_4OH solution (30 mL). The crystals were then dried overnight, then taken up in absolute EtOH (30 mL) and concentrated HCl (5 mL), and to the pale yellow solution was added finely granulated tin (2.98 g, 25.1 mmol). The mixture was heated at reflux for 16 h, then filtered to remove any remaining tin, then concentrated in vacuo. Water (20 mL) and NH_4OH solution were added until the mixture became alkaline, which caused a white precipitate to form. The product was extracted with EtOAc (3 × 30 mL) and the combined organic extracts washed with brine (20 mL), dried over anhydrous Na_2SO_4, filtered through a sinter funnel to remove any remaining precipitates, then evaporated to dryness to give the product as a pale yellow oil (764 mg, 85%). ^{1}H NMR δ 7.09–7.02 (m, 2H), 6.66–6.59 (m, 2H), 4.12 (q, J = 7.1 Hz, 2H), 3.58 (br s, 2H), 3.48 (s, 2H), 1.24 (t, J = 7.1 Hz, 3H). ^{13}C NMR δ 172.3 (C), 145.5 (C), 130.2 (CH), 124.1 (C), 115.3 (CH), 60.8 (CH_2), 40.7 (CH_2), 14.3 (CH_3).

Ethyl 2-(4-((tert-butoxycarbonyl)amino)phenyl)acetate (**21**).[48] Using **20** (700 mg, 3.91 mmol) as the starting material, following General Procedure A. The product was purified by flash column chromatography (petroleum spirits/EtOAc, 6:1) to give the title compound as a colourless oil which slowly crystallised (833 mg, 76%). ^{1}H NMR δ 7.31 (d, J = 8.4 Hz, 2H), 7.20 (d, J = 8.5 Hz, 2H), 6.50 (br s, 1H) 4.13 (q, J = 7.1 Hz, 2H), 3.55 (s, 2H), 1.51 (s, 9H), 1.24 (t, J = 7.1 Hz, 3H). ^{13}C NMR δ 171.2 (C), 151.4 (C), 137.5 (C), 129.9 (CH), 128.8 (C), 118.8 (CH), 80.9 (C), 61.0 (CH_2), 40.9 (CH_2), 28.5 (CH_3), 14.3 (CH_3).

tert-*Butyl (4-(2-oxoethyl)phenyl)carbamate* (**22**).[45] Using **21** (414 mg, 1.48 mmol) as the starting material, following General Procedure B, gave the title compound as a colourless oil which slowly solidified (347 mg, 99%). ^{1}H NMR δ 9.71 (t, *J* = 2.4 Hz, 1H), 7.37 (d, *J* = 8.4 Hz, 2H), 7.13 (d, *J* = 8.5 Hz, 2H), 6.53 (s, 1H), 3.63 (d, *J* = 2.4 Hz, 2H), 1.52 (s, 9H). ^{13}C NMR δ 199.6 (CH), 152.6 (C), 137.9 (C), 130.3 (CH), 126.3 (C), 119.2 (CH), 80.2 (C), 50.0 (CH_2), 28.5 (CH_3).

7-Nitro-1,2,3,4-tetrahydroisoquinoline hydrochloride (**24**).[49] 1,2,3,4-Tetrahydroisoquinoline (**23**, 10.0 g, 75.1 mmol) was added dropwise to ice cold concentrated sulfuric acid (40 mL), and sodium nitrate (7.66 g, 90.1 mmol) was carefully added so as not to reach above 5 °C. The solution was allowed to warm to RT, and was stirred for 20 h. The mixture was then cooled on ice, diluted with water (80 mL), and conc. NH_4OH solution was added to pH 10, causing a brown precipitate which was extracted with $CHCl_3$ (3 × 40 mL). The combined organic extracts were washed with brine (40 mL), dried over anhydrous Na_2SO_4 and evaporated to dryness. The orange oil was taken up in EtOH (100 mL), cooled on ice and concentrated HCl (20 mL) added to force the slow precipitation of the HCl salt as a yellow solid. The product was filtered, then recrystallised from CH_3OH and washed with acetone to reveal the title compound as pale brown needles. A second recrystallisation in aqueous acetone revealed the product as white needles (4.82 g, 30%) ^{1}H NMR (d_6-DMSO) δ 10.08 (br s, 2H), 8.22 (d, *J* = 2.3 Hz, 1H), 8.09 (dd, *J* = 8.5, 2.5 Hz, 1H), 7.53 (d, *J* = 8.5 Hz, 1H), 4.38 (s, 2H), 3.38 (t, *J* = 6.2 Hz, 2H), 3.17 (t, *J* = 6.1 Hz, 2H). ^{13}C NMR (d_6-DMSO) δ 145.9 (C), 140.4 (C), 131.1 (C), 130.2 (CH), 122.0 (CH), 121.9 (CH), 43.1 (CH_2), 39.8 (CH_2), 24.9 (CH_2).

1-(2,3-Dichlorophenyl)-1,4-diazepane (**26**).[11] To a solution of 2,2'-bis(diphenylphosphino)-1,1'-binaphthalene (110 mg, 177 μmol) in degassed toluene (45 mL) was added tris(dibenzylideneacetone)dipalladium (162 mg, 177 μmol) and potassium *tert*-butoxide (2.98

g, 26.6 mmol). 1-Bromo-2,3-dichlorobenzene (**25**, 2.00 g, 8.85 mmol) and homopiperazine (1.77 g, 17.7 mmol) were added and the brown mixture heated to 80 °C for 24 h. After cooling to RT, a solution of di-*tert*-butyl dicarbonate (5.80 g, 26.6 mmol) in toluene (5 mL) was slowly added to the mixture and it was stirred at RT for 2 h. Water (20 mL) was added to quench the reaction, and the mixture was extracted with EtOAc (3 × 25 mL). The combined organic extracts were washed with brine (20 mL), dried over anhydrous Na_2SO_4 and evaporated to dryness to give an orange oil. *tert*-Butyl 4-(2,3-dichlorophenyl)-1,4-diazepane-1-carboxylate was then purified by flash column chromatography (petroleum spirits/EtOAc, 9:1). The yellow oil was taken up in DCM (5 mL) and TFA (1 mL) and stirred at RT. After 90 min, 10% NH_4OH solution (2 mL) was added, then the product extracted with DCM (2 × 20 mL), and the combined organic extracts washed with brine (10 mL), dried over anhydrous Na_2SO_4 and evaporated to dryness to give the title compound as an orange oil (54 mg, 3%). ^{1}H NMR δ 7.11–7.06 (m, 2H), 7.04–6.99 (m, 1H), 3.33–3.20 (m, 4H), 3.12–2.99 (m, 4H), 2.09 (br s, 1H), 1.99–1.89 (m, 2H). ^{13}C NMR δ 153.6 (C), 134.0 (C), 127.5 (C), 127.2 (CH), 123.9 (CH), 120.1 (CH), 57.9 (CH_2), 54.6 (CH_2), 49.9 (CH_2), 47.9 (CH_2), 31.4 (CH_2). LCMS (*m*/*z*): 245.1 $[M+H]^+$.

General Procedure C (Reductive Alkylation)

The aldehyde (1 equiv) and amine (1 equiv) were taken up in 1,2-DCE (10 mL). $NaBH(OAc)_3$ (1.5 equiv) was added to the stirred solution at RT under nitrogen. After 16–24 h LCMS confirmed reaction completion. The mixture was diluted with DCM (15 mL), washed with 1 M K_2CO_3 solution (3 × 20 mL), brine (15 mL), then dried over anhydrous Na_2SO_4 and evaporated to dryness. The crude material was purified by flash column chromatography to give the title compound.

tert-*Butyl (*trans-*4-(2-(3,4-dihydroisoquinolin-2(1*H*)-yl)ethyl)cyclohexyl)carbamate* (**4**). Using **16** (150 mg, 622 μmol) as the aldehyde, and **23** (82.8 mg, 622 μmol) as the amine

following General Procedure C. Eluted with EtOAc to give the title compound as a white wax (190 mg, 85%). mp: 110-111 °C. ^{1}H NMR δ 7.16–7.05 (m, 3H), 7.04–6.97 (m, 1H), 4.39 (br s, 1H), 3.60 (s, 2H), 3.38 (br s, 1H), 2.89 (t, *J* = 5.9 Hz, 2H), 2.71 (t, *J* = 5.9 Hz, 2H), 2.53–2.50 (m, 2H), 2.02–1.94 (m, 2H), 1.84–1.72 (m, 2H), 1.55–1.45 (m, 2H), 1.44 (s, 9H), 1.33–1.20 (m, 1H), 1.13–0.97 (m, 4H). ^{13}C NMR δ 155.4 (C), 134.9 (C), 134.4 (C), 128.7 (CH), 126.7 (CH), 126.2 (CH), 125.7 (CH), 79.1 (C), 56.4 (CH_2), 56.3 (CH_2), 51.1 (CH_2), 50.0 (CH), 35.4 (CH), 34.3 (CH_2), 33.6 (CH_2), 32.1 (CH_2), 29.2 (CH_2), 28.6 (CH_3). HPLC t_R = 8.93 min, 99% purity. HRMS (*m/z*): $[MH]^+$ calcd. for $C_{22}H_{34}N_2O_2$, 359.2693; found 359.2711.

tert-*Butyl (*trans-*4-(2-(7-nitro-3,4-dihydroisoquinolin-2(1*H*)-yl)ethyl)cyclohexyl)carbamate* (**29**). Using **16** (162 mg, 671 μmol) as the aldehyde, and **24** (119 mg, 671 μmol) as the amine following General Procedure C. Eluted with EtOAc, to give the title compound as pale yellow flakes (213 mg, 79%). mp: 137-138 °C. ^{1}H NMR δ 7.97 (dd, *J* = 8.4, 2.4 Hz, 1H), 7.92 (d, *J* = 2.2 Hz, 1H), 7.24 (d, *J* = 8.4 Hz, 1H), 4.38 (br s, 1H), 3.68 (s, 2H), 3.38 (br s, 1H), 2.98 (t, *J* = 5.8 Hz, 2H), 2.75 (t, *J* = 5.9 Hz, 2H), 2.61–2.50 (m, 2H), 2.04–1.92 (m, 2H), 1.85–1.72 (m, 2H), 1.53–1.46 (m, 2H), 1.45 (s, 9H), 1.36–1.22 (m, 1H), 1.17–0.97 (m, 4H). ^{13}C NMR δ 155.37 (C), 146.2 (C), 142.6 (C), 136.6 (C), 129.7 (CH), 121.9 (CH), 121.3 (CH), 79.1 (C), 56.1 (CH_2), 55.9 (CH_2), 50.3 (CH_2), 50.0 (CH), 35.3 (CH), 34.1 (CH_2), 33.5 (CH_2), 32.1 (CH_2), 29.5 (CH_2), 28.6 (CH_3). HPLC t_R = 9.01 min, 95% purity. HRMS (*m/z*): $[MH]^+$ calcd. for $C_{22}H_{33}N_3O_4$, 404.2544; found 404.2549.

tert-*Butyl (*trans-*4-(2-(7-cyano-3,4-dihydroisoquinolin-2(1*H*)-yl)ethyl)cyclohexyl)carbamate* (**30**).[15] Using **16** (215 mg, 891 μmol) as the aldehyde, and **27** (141 mg, 891 μmol) as the amine following General Procedure C. Eluted with EtOAc to give the title compound as white needles (193 mg, 56%). mp: 294-296 °C. ^{1}H NMR δ 7.39 (dd, *J* = 7.9, 1.6 Hz, 1H), 7.32 (s, 1H), 7.18 (d, *J* = 7.9 Hz, 1H), 4.37 (br s, 1H), 3.60 (s, 2H), 3.37

(br s, 1H), 2.94 (t, J = 5.8 Hz, 2H), 2.72 (t, J = 5.9 Hz, 2H), 2.57–2.49 (m, 2H), 2.05–1.94 (m, 2H), 1.82–1.74 (m, 2H), 1.53–1.40 (m, 11H), 1.32–1.22 (m, 1H), 1.14–0.98 (m, 4H). ^{13}C NMR δ 155.2 (C), 140.3 (C), 136.3 (C), 130.3 (CH), 129.5 (CH), 129.4 (CH), 119.0 (C), 109.2 (C), 78.8 (C), 56.0 (CH_2), 55.5 (CH_2), 50.2 (CH_2), 49.8 (CH), 35.1 (CH), 34.0 (CH_2), 33.3 (CH_2), 31.9 (CH_2), 29.4 (CH_2), 28.4 (CH_3). HPLC t_R = 8.76 min, 98% purity. HRMS (*m/z*): $[MH]^+$ calcd. for $C_{22}H_{33}N_3O_2$, 384.2646; found 384.2645.

tert-*Butyl* (trans-*4-(2-(4-(2,3-dichlorophenyl)-1,4-diazepan-1-yl)ethyl)cyclohexyl)carbamate* (**31**).[50] Using **16** (50 mg, 207 µmol) and **26** (56 mg, 228 µmol) as the amine following General Procedure C. Purification by flash column chromatography ($CHCl_3/CH_3OH$, 50:1 to 20:1) gave the title compound as a pale yellow oil (48 mg, 49%). ^{1}H NMR δ 7.12–7.05 (m, 2H), 7.03–6.96 (m, 1H), 4.37 (br s, 1H), 3.43–3.20 (m, 5H), 2.87 (br s, 4H), 2.66–2.53 (m, 2H), 2.08–1.90 (m, 4H), 1.83–1.70 (m, 2H), 1.50–1.39 (m, 11H), 1.30–1.18 (m, 1H), 1.13–0.96 (m, 4H). ^{13}C NMR δ 155.3 (C), 153.0 (C), 134.1 (C), 127.1 (CH), 127.0 (C), 123.9 (CH), 119.9 (CH), 79.1 (C), 56.3 (CH_2), 56.2 (CH_2), 54.6 (CH_2), 54.2 (CH_2), 53.4 (CH_2), 50.0 (CH), 35.5 (CH), 34.2 (CH_2), 33.6 (CH_2), 32.1 (CH_2), 28.6 (CH_3), 27.8 (CH_2). HPLC t_R = 10.18 min, >99% purity. HRMS (*m/z*): $[MH]^+$ calcd. for $C_{24}H_{37}Cl_2N_3O_2$, 470.2336; found 470.2345.

tert-*Butyl* (trans-*4-(2-(4-(2,3-dichlorophenyl)piperazin-1-yl)ethyl)cyclohexyl)carbamate* (**32**).[12] Using **16** (200 mg, 829 µmol) as the aldehyde and **28** (230 mg, 995 µmol) as the amine following General Procedure C. Purification by flash column chromatography (petroleum spirits/EtOAc, 5:1) gave the title compound as a white wax (262 mg, 69%). mp: 143-145 °C. ^{1}H NMR δ 7.17–7.10 (m, 2H), 6.99–6.92 (m, 1H), 4.37 (br s, 1H), 3.37 (br s, 1H), 3.07 (br s, 4H), 2.62 (br s, 4H), 2.48–2.38 (m, 2H), 2.04–1.92 (m, 2H), 1.82–1.73 (m, 2H), 1.49–1.37 (m, 11H), 1.30–1.17 (m, 1H), 1.15–0.97 (m, 4H). ^{13}C NMR δ 155.3 (C), 151.5 (C), 134.2 (C), 127.64 (C), 127.56 (CH), 124.7 (CH), 118.7 (CH), 79.2 (C), 56.7

(CH_2), 53.5 (CH_2), 51.5 (CH_2), 50.0 (CH), 35.6 (CH), 34.0 (CH_2), 33.6 (CH_2), 32.1 (CH_2), 28.6 (CH_3). HPLC t_R = 9.62 min, >99% purity. HRMS (*m/z*): $[MH]^+$ calcd. for $C_{23}H_{35}Cl_2N_3O_2$, 456.2179; found 456.2195.

General Procedure D (Deprotection of *tert*-Butyl Carbamate)

The protected amine (250 μmol) was taken up in DCM (5 mL) and to the stirred solution at RT was added TFA (2 mL). The solution was stirred for 2–16 h, then diluted with DCM (20 mL). Water (20 mL) and ammonium hydroxide solution (5 mL) were added to achieve pH 10. The product was then extracted with DCM (2 × 20 mL), and the combined organic extracts washed with brine (20 mL), then dried over anhydrous Na_2SO_4 and evaporated to dryness to give the free amine.

trans-*4-(2-(3,4-Dihydroisoquinolin-2(1*H*)-yl)ethyl)cyclohexanamine dihydrochloride* (**33**). Using **4** as the starting material, following Procedure D, the product was converted to the dihydrochloride salt by the addition of 1 M HCl in Et_2O, followed by removal of solvents to give the title compound as white prisms (80%). ^{1}H NMR (D_2O) δ 7.64–7.54 (m, 3H), 7.51–7.49 (m, 1H), 4.84–4.79 (m, 1H), 4.54 (d, *J* = 15.5 Hz, 1H), 4.07–3.96 (m, 1H), 3.65–3.26 (m, 6H), 2.27 (d, *J* = 10.7 Hz, 2H), 2.11 (d, *J* = 11.8 Hz, 2H), 1.99 (dt, *J* = 11.0, 5.6 Hz, 2H), 1.70–1.55 (m, 3H), 1.45–1.26 (m, 2H). ^{13}C NMR (D_2O) δ 132.1 (C), 130.0 (CH), 129.6 (CH), 128.8 (C), 128.4 (CH), 128.0 (CH), 55.3 (CH_2), 53.6 (CH_2), 50.8 (CH), 50.7 (CH_2), 34.6 (CH), 31.01 (3 × CH_2), 30.96 (2 × CH_2), 26.1 (CH_2). HPLC t_R = 5.07 min, 99% purity. HRMS (*m/z*): $[MH]^+$ calcd. for $C_{19}H_{27}N_2$, 259.2169; found 259.2167.

*2-(2-(*trans-*4-Aminocyclohexyl)ethyl)-1,2,3,4-tetrahydroisoquinoline-7-carbonitrile dihydrochloride* (**34**). Starting with **30**, following Procedure D, the product was converted to the dihydrochloride salt by the addition of 1 M HCl in Et_2O, followed by removal of solvents to give the title compound as a white solid (92%). ^{1}H NMR (CD_3OD) δ 7.68–7.62 (m, 2H), 7.48–7.43 (m, 1H), 4.50 (s, 2H), 3.61 (s, 2H), 3.39–3.24 (m, 4H), 3.08 (tt, *J* = 11.9, 4.0 Hz,

1H), 2.13–2.02 (m, 2H), 1.99–1.89 (m, 2H), 1.86–1.75 (m, 2H), 1.52–1.37 (m, 3H), 1.19 (qd, J = 13.3, 3.1 Hz, 2H). ^{13}C NMR (CD_3OD) δ 138.5 (C), 132.5 (CH), 131.9 (CH), 131.3 (C), 131.1 (CH), 119.2 (C), 112.0 (C), 56.0 (CH_2), 53.5 (CH_2), 51.4 (CH), 50.6 (CH_2), 35.4 (CH), 31.7 (CH_2), 31.6 (CH_2), 31.5 (CH_2), 27.0 (CH_2). HPLC t_R = 5.04 min, 99% purity. HRMS (*m/z*): $[MH]^+$ calcd. for $C_{18}H_{25}N_3$, 284.2121; found 284.2133.

General Procedure E (Acetamide Synthesis)

The amine starting material (175 µmol) was taken up in DCM (3 mL), *N,N*-diisopropylethylamine (76 µL, 438 µmol) and acetic anhydride (18 µL, 193 µmol) and the clear solution stirred at RT for 2h. The mixture was then concentrated *in vacuo*, diluted with water (10 mL) and made alkaline with the addition of NH_4OH solution (5 mL). The product was extracted with $CHCl_3$ (3 × 15 mL) and the combined organic extracts washed with brine (15 mL), dried over anhydrous Na_2SO_4, and evaporated to dryness.

N-*(*trans-*4-(2-(3,4-Dihydroisoquinolin-2(1*H*)-yl)ethyl)cyclohexyl)acetamide* (**35**). Using **33** as the amine following General Procedure E, the crude material was crystallised (CH_3OH/H_2O) to reveal the title compound as a white solid (87%). mp: 257-259 °C. ^{1}H NMR δ 7.14–7.04 (m, 3H), 7.04–6.95 (m, 1H), 5.66 (d, J = 8.0 Hz, 1H), 3.71–3.67 (m, 1H), 3.60 (s, 2H), 2.89 (t, J = 5.8 Hz, 2H), 2.70 (t, J = 5.9 Hz, 2H), 2.55–2.44 (m, 2H), 2.01–1.89 (m, 5H), 1.84–1.71 (m, 2H), 1.55–1.43 (m, 2H), 1.33–1.24 (m, 1H), 1.13–0.97 (m, 4H). ^{13}C NMR δ 169.3 (C), 134.9 (C), 134.4 (C), 128.6 (CH), 126.6 (CH), 126.1 (CH), 125.6 (CH), 56.3 (2 × CH_2), 51.1 (CH_2), 48.7 (CH), 35.3 (CH), 34.2 (CH_2), 33.1 (CH_2), 31.9 (CH_2), 29.1 (CH_2), 23.5 (CH_3). HPLC (214 nm) t_R = 6.72 min, 96% purity. HRMS (*m/z*): $[MH]^+$ calcd. for $C_{19}H_{28}N_2O$, 301.2274; found 301.2274.

N-*(*trans-*4-(2-(7-Cyano-3,4-dihydroisoquinolin-2(1*H*)-yl)ethyl)cyclohexyl)acetamide* (**36**). Using **34** as the amine following General Procedure E, the crude material was purified by flash column chromatography ($CHCl_3/CH_3OH$, 5:1) to give the title compound as white

needles (26%). mp: 241-243 °C. ^{1}H NMR δ 7.39 (dd, *J* = 7.9, 1.6 Hz, 1H), 7.32 (br s, 1H), 7.19 (d, *J* = 7.9 Hz, 1H), 5.40 (d, *J* = 8.0 Hz, 1H), 3.77–3.64 (m, 1H), 3.60 (s, 2H), 2.94 (t, *J* = 5.8 Hz, 2H), 2.72 (t, *J* = 5.9 Hz, 2H), 2.56–2.50 (m, 2H), 2.06–1.87 (m, 5H), 1.86–1.76 (m, 2H), 1.53–1.45 (m, 2H), 1.35–1.23 (m, 1H), 1.18–1.02 (m, 4H). ^{13}C NMR δ 169.4 (C), 140.5 (C), 136.4 (C), 130.5 (CH), 129.7 (CH), 129.6 (CH), 119.2 (C), 109.5 (C), 56.1 (CH_2), 55.7 (CH_2), 50.3 (CH_2), 48.8 (CH), 35.3 (CH), 34.1 (CH_2), 33.1 (CH_2), 31.9 (CH_2), 29.5 (CH_2), 23.7 (CH_3). HPLC t_R = 6.65 min, 96% purity. HRMS (*m/z*): $[MH]^+$ calcd. for $C_{20}H_{28}N_3O$, 326.2227; found 326.2213.

*Ethyl (*trans-*4-(2-(3,4-dihydroisoquinolin-2(1*H*)-yl)ethyl)cyclohexyl)carbamate* (**37**). **33** (120 mg, 464 µmol) was taken up in DCM (10 mL) and Et_3N (129 µL, 929 µmol) at RT, and diethyl pyrocarbonate (82 µL, 557 µmol) slowly added. After 14 h, LCMS suggested reaction completion. The mixture was concentrated *in vacuo* then purified by recrystallization (CH_3OH/H_2O) to give the title compound as a pale yellow solid (135 mg, 88%). ^{1}H NMR δ 7.15–7.06 (m, 3H), 7.04–6.98 (m, 1H), 4.49 (br s, 1H), 4.09 (q, *J* = 6.3 Hz, 2H), 3.64–3.57 (m, 2H), 3.43–3.38 (m, 1H), 2.90 (t, *J* = 5.8 Hz, 2H), 2.71 (t, *J* = 5.9 Hz, 2H), 2.53–2.48 (m, 2H), 2.05–1.95 (m, 2H), 1.82–1.78 (m, 2H), 1.58–1.43 (m, 3H), 1.31–1.19 (m, 3H), 1.17–1.00 (m, 4H). ^{13}C NMR δ 156.0 (C), 134.9 (C), 134.4 (C), 128.7 (CH), 126.7 (CH), 126.2 (CH), 125.7 (CH), 60.7 (CH_2), 56.4 (CH_2), 56.4 (CH_2), 51.1 (CH_2), 50.8 (CH), 35.4 (CH), 34.2 (CH_2), 33.5 (CH_2), 32.0 (CH_2), 29.8 (CH_2), 29.1 (CH_3). The compound was further purified prior to pharmacological analysis by preparative HPLC to give the title compound as the trifluoroacetate as a clear oil. HPLC t_R = 7.60 min, >99% purity. *m/z* (ESI 20 V) 331.2 (MH^+). HRMS (*m/z*): $[MH]^+$ calcd. for $C_{20}H_{30}N_2O_2$, 331.2380; found 331.2379.

*Isopropyl (*trans-*4-(2-(3,4-dihydroisoquinolin-2(1*H*)-yl)ethyl)cyclohexyl)carbamate* (**38**). **33** (40 mg, 155 µmol) was taken up in CH_3CN (5 mL) and DCM (5 mL), and to the stirred solution at RT was added 1,1'-carbonyldiimidazole (25 mg, 155 µmol). The colourless

mixture was stirred overnight under nitrogen, and after 16 h, isopropanol (1 mL) was added. The solution was stirred for a further 16 h. To force reaction progression, further isopropanol (10 mL) was added, and the solution heated to reflux overnight. After 16 h, the mixture was evaporated to dryness in vacuo, then purified by flash column chromatography ($CHCl_3/CH_3OH$, 100:1 to 20:1) to give the title compound as a white wax (11 mg, 23%). ^{1}H NMR δ 7.16–7.05 (m, 3H), 7.04–6.97 (m, 1H), 4.89 (dt, *J* = 12.2, 5.9 Hz, 1H), 4.43 (d, *J* = 5.9 Hz, 1H), 3.63 (s, 2H), 3.42 (br s, 1H), 2.91 (t, *J* = 5.8 Hz, 2H), 2.74 (t, *J* = 5.9 Hz, 2H), 2.58–2.47 (m, 2H), 2.02–1.98 (m, 2H), 1.86–1.73 (m, 2H), 1.52 (dd, *J* = 15.3, 6.9 Hz, 2H), 1.33–1.17 (m, 7H), 1.15–0.99 (m, 4H). ^{13}C NMR δ 155.5 (C), 134.5 (C), 134.2 (C), 128.8 (CH), 126.7 (CH), 126.3 (CH), 125.8 (CH), 67.8 (CH), 56.3 (CH_2), 56.2 (CH_2), 51.1 (CH_2), 50.2 (CH), 35.4 (CH), 34.2 (CH_2), 33.5 (CH_2), 32.0 (CH_2), 29.0 (CH_2), 22.3 (CH_3). HPLC t_R = 8.02 min, 99% purity. HRMS (*m/z*): $[MH]^+$ calcd. for $C_{21}H_{32}N_2O_2$, 345.2537; found 345.2546.

*Isobutyl (*trans*-4-(2-(3,4-dihydroisoquinolin-2(1*H*)-yl)ethyl)cyclohexyl)carbamate* (**39**). **33** (40 mg, 155 μmol) was taken up in DCM (5 mL) and Et_3N (43 μL, 310 μmol), and to the stirred solution at RT under nitrogen was slowly added isobutyl chloroformate (40 μL, 310 μmol). After 1 h, the solution was diluted with DCM (20 mL), washed with water (20 mL), 1 M $KHSO_4$ solution (15 mL), brine (15 mL), then dried over anhydrous Na_2SO_4 and evaporated to dryness. The product was purified by flash column chromatography ($CHCl_3/CH_3OH$, 30:1) to give the title compound as a white solid (27 mg, 49%). mp: 99-100 °C. ^{1}H NMR δ 7.14–7.06 (m, 3H), 7.04–6.98 (m, 1H), 4.48 (d, *J* = 5.1 Hz, 1H), 3.82 (d, *J* = 6.2 Hz, 2H), 3.61 (s, 2H), 3.42 (br s, 1H), 2.90 (t, *J* = 5.9 Hz, 2H), 2.71 (t, *J* = 5.9 Hz, 2H), 2.57–2.46 (m, 2H), 2.05–1.96 (m, 2H), 1.88 (m, 1H), 1.85–1.76 (m, 2H), 1.55–1.47 (m, 2H), 1.35–1.21 (m, 1H), 1.17–1.00 (m, 4H), 0.92 (d, *J* = 6.7 Hz, 6H). ^{13}C NMR δ 156.2 (C), 135.0 (C), 134.5 (C), 128.8 (CH), 126.7 (CH), 126.2 (CH), 125.7 (CH), 70.9 (CH_2), 56.4 (CH_2),

56.4 (CH_2), 51.2 (CH_2), 50.3 (CH), 35.4 (CH), 34.3 (CH_2), 33.6 (CH_2), 32.1 (CH_2), 29.2 (CH_2), 28.2 (CH), 19.2 (CH_3). HPLC t_R = 8.52 min, >99% purity. HRMS (*m/z*): $[MH]^+$ calcd. for $C_{22}H_{34}N_2O_2$, 359.2693; found 359.2693.

*Phenyl (*trans-*4-(2-(3,4-dihydroisoquinolin-2(1*H*)-yl)ethyl)cyclohexyl)carbamate* (**40**). **33** (110 mg, 426 µmol) was taken up in DCM (10 mL) and *N,N*-diisopropylethylamine (148 µL, 851 µmol). To the stirred solution at RT was slowly added phenyl chloroformate (64 µL, 511 µmol). After 14 h, LCMS confirmed reaction completion. The mixture was diluted with DCM (15 mL), washed with water (15 mL), brine (15 mL), then organic extracts dried over anhydrous Na_2SO_4 and evaporated to dryness to reveal a white solid. The title compound was then purified by flash column chromatography (petroleum spirits/EtOAc, 1:1) to give the title compound as a white solid (145 mg, 90%). mp: 157-158 °C. ^{1}H NMR δ 7.39–7.30 (m, 2H), 7.22–7.06 (m, 6H), 7.05–6.98 (m, 1H), 4.92 (d, *J* = 7.9 Hz, 1H), 3.63 (s, 2H), 3.57–3.42 (m, 1H), 2.90 (t, *J* = 5.6 Hz, 2H), 2.73 (t, *J* = 6.0 Hz, 1H), 2.59–2.46 (m, 2H), 2.12–2.16 (m, 2H), 1.86–1.80 (m, 2H), 1.56–1.41 (m, 2H), 1.41–1.21 (m, 1H), 1.19–0.94 (m, 4H). ^{13}C NMR δ 153.9 (C), 151.2 (C), 134.8 (C), 134.4 (C), 129.3 (CH), 128.8 (CH), 126.7 (CH), 126.2 (CH), 125.7 (CH), 125.2 (CH), 121.7 (CH), 56.3 (2 × CH_2), 51.1 (CH_2), 50.7 (CH), 35.3 (CH), 34.1 (CH_2), 33.3 (CH_2), 31.9 (CH_2), 29.1 (CH_2). HPLC t_R = 8.71 min, >99 % purity. HRMS (*m/z*): $[MH]^+$ calcd. for $C_{24}H_{30}N_2O_2$, 379.2380; found 379.2388.

*3-(*trans-*4-(2-(3,4-Dihydroisoquinolin-2(1*H*)-yl)ethyl)cyclohexyl)-1,1-dimethylurea* (**41**). **33** (40 mg, 155 µmol) was taken up in THF (5 mL) under N_2, and to the stirred solution was added 1,1′-carbonyldiimidazole (125 mg, 774 µmol) and *N,N*-diisopropylethylamine (270 µL, 1.55 mmol). This was stirred at RT for 30 min, then dimethylamine hydrochloride (126 mg, 1.55 mmol) was added, and the mixture stirred for 16 h. LCMS confirmed the complete consumption of starting material, and the reaction was quenched with 10% NH_4OH solution (20 mL). The product was then extracted with DCM (2 × 20 mL), and the combined organic

extracts washed with brine (20 mL), dried over anhydrous Na_2SO_4 and evaporated to dryness. The crude product was purified by flash column chromatography ($CHCl_3/CH_3OH$, 10:1) to give the title compound as a white solid (42 mg, 82%). mp: 130-131 °C. ^{1}H NMR δ 7.16–7.06 (m, 3H), 7.04–6.99 (m, 1H), 4.12 (d, *J* = 7.6 Hz, 1H), 3.65 (s, 2H), 3.62–3.53 (m, 1H), 2.96–2.83 (m, 8H), 2.76 (t, *J* = 6.0 Hz, 2H), 2.60–2.51 (m, 2H), 2.05–1.96 (m, 2H), 1.87–1.76 (m, 2H), 1.57–1.47 (m, 2H), 1.33–1.24 (m, 1H), 1.17–0.98 (m, 4H). ^{13}C NMR δ 158.0 (C), 134.5 (C), 134.3 (C), 128.8 (CH), 126.7 (CH), 126.3 (CH), 125.8 (CH), 56.2 (CH_2), 56.0 (CH_2), 50.9 (CH_2), 50.0 (CH), 36.3 (CH_3), 35.6 (CH), 34.1 (CH_2), 34.0 (CH_2), 32.2 (CH_2), 28.8 (CH_2). HPLC t_R = 6.88 min, >99% purity. HRMS (*m/z*): $[MH]^+$ calcd. for $C_{20}H_{31}Cl_2N_3O$, 330.2540; found 330.2551.

*1-(*tert*-Butyl)-3-(*trans*-4-(2-(3,4-dihydroisoquinolin-2(1*H*)-yl)ethyl)cyclohexyl)urea* (**42**). **33** (110 mg, 426 µmol), was taken up in CH_3CN (10 mL), and 1,1′-carbonyldiimidazole (76 mg, 468 µmol) and Et_3N (297 µL, 2.13 mmol) were added to the stirred solution at RT. The solution was then heated at 60 °C for 30 min, then *tert*-butylamine (89 µL, 851 µmol) added, and the solution stirred at RT for 16 h. The mixture was then evaporated to dryness and purified by recrystallization (CH_3OH/H_2O) to give the title compound as a white solid (59 mg, 43%). ^{1}H NMR δ 7.15–7.05 (m, 3H), 7.04–6.97 (m, 1H), 4.18 (s, 1H), 4.05 (d, *J* = 8.0 Hz, 1H), 3.60 (s, 2H), 3.44 (m, 1H), 2.89 (t, *J* = 5.6 Hz, 2H), 2.71 (t, *J* = 6.0 Hz, 2H), 2.54–2.45 (m, 2H), 2.02–1.95 (m, 2H), 1.83–1.77 (m, 2H), 1.52–1.44 (m, 2H), 1.32 (s, 9H), 1.31–1.19 (m, 1H), 1.14–0.97 (m, 4H). ^{13}C NMR δ 157.0 (C), 135.1 (C), 134.5 (C), 128.8 (CH), 126.7 (CH), 126.2 (CH), 125.7 (CH), 56.5 (CH_2), 56.4 (CH_2), 51.2 (CH_2), 50.5 (C), 49.5 (CH), 35.5 (CH), 34.3 (CH_2), 34.1 (CH_2), 32.2 (CH_2), 29.7 (CH_3), 29.3 (CH_2). The compound was further purified prior to pharmacological analysis by preparative HPLC to give the title compound as the trifluoroacetate as a clear oil. HPLC t_R = 7.86 min, 99% purity. HRMS (*m/z*): $[MH]^+$ calcd. for $C_{22}H_{35}N_3O$, 358.2853; found 358.2855.

*tert-Butyl (*trans-*4-((3,4-dihydroisoquinolin-2(1*H*)-yl)methyl)cyclohexyl)carbamate* (**43**). Using **17** (43 mg, 189 μmol) as the aldehyde, and **23** (28 mg, 208 μmol) as the amine following General Procedure C. Purification by flash column chromatography (petroleum spirits/EtOAc, 1:1) gave a pale yellow oil which was further purified by flash column chromatography (petroleum spirits/EtOAc, 1:1) to give the title compound as a white wax (47 mg, 72%). ^{1}H NMR δ 7.13–7.05 (m, 3H), 7.03–6.97 (m, 1H), 4.41 (br s, 1H), 3.57 (s, 2H), 3.40 (br s, 1H), 2.88 (t, *J* = 5.8 Hz, 2H), 2.67 (t, *J* = 5.9 Hz, 2H), 2.30 (d, *J* = 7.1 Hz, 2H), 2.06–1.94 (m, 2H), 1.94–1.81 (m, 2H), 1.58–1.47 (m, 1H), 1.47–1.39 (m, 9H), 1.16–0.93 (m, 4H). ^{13}C NMR δ 155.4 (C), 135.1 (C), 134.6 (C), 128.8 (CH), 126.7 (CH), 126.1 (CH), 125.6 (CH), 79.1 (C), 64.9 (CH_2), 56.8 (CH_2), 51.4 (CH_2), 50.2 (CH), 34.8 (CH), 33.4 (CH_2), 30.6 (CH_2), 29.2 (CH_2), 28.6 (CH_3). HPLC t_R = 7.84 min, 95% purity. HRMS (*m/z*): $[MH]^+$ calcd. for $C_{21}H_{32}N_2O_2$, 345.2537; found 345.2533.

tert-*butyl ((*trans-*4-((3,4-dihydroisoquinolin-2(1*H*)-yl)methyl)cyclohexyl)methyl)carbamate* (**44**). Using **18** (230 mg, 953 μmol) as the aldehyde and **23** (152 mg, 1.14 mmol) as the amine following General Procedure C. Purification by flash column chromatography (petroleum spirits/EtOAc, 4:1) gave the title compound as a colourless oil (75 mg, 22%). ^{1}H NMR δ 7.13–7.05 (m, 3H), 7.03–6.97 (m, 1H), 4.59 (s, 1H), 3.57 (s, 2H), 2.97 (t, *J* = 6.0 Hz, 2H), 2.88 (t, *J* = 5.7 Hz, 2H), 2.69–2.64 (m, 2H), 2.30 (d, *J* = 7.1 Hz, 2H), 1.89 (m, 2H), 1.77 (m, 2H), 1.63–1.49 (m, 1H), 1.46–1.42 (m, 10H), 1.02–0.83 (m, 4H). ^{13}C NMR δ 156.2 (C), 135.3 (C), 134.7 (C), 128.8 (CH), 126.7 (CH), 126.1 (CH), 125.6 (CH), 79.1 (C), 65.5 (CH_2), 56.9 (CH_2), 51.4 (CH_2), 47.0 (CH_2), 38.8 (CH), 35.6 (CH), 31.4 (CH_2), 30.5 (CH_2), 29.3 (CH_2), 28.6 (CH_3). HPLC t_R = 9.82 min, >99% purity. HRMS (m/z): $[MH]^+$ calcd. for $C_{22}H_{34}N_2O_2$, 359.2693; found 359.2708.

tert-*Butyl (*cis-*4-(2-(3,4-dihydroisoquinolin-2(1*H*)-yl)ethyl)cyclohexyl)carbamate* (**45**). Using **19** (280 mg, 1.16 mmol) as the aldehyde and **23** (185 mg, 1.39 mmol) as the amine

following General Procedure C. Eluted with EtOAc to give the title compound as a pale yellow oil (263 mg, 63%). ^{1}H NMR δ 7.16–7.06 (m, 3H), 7.05–6.97 (m, 1H), 4.64 (br s, 1H), 3.75–3.65 (m, 1H), 3.62 (s, 2H), 2.90 (t, *J* = 5.9 Hz, 2H), 2.72 (t, *J* = 5.9 Hz, 2H), 2.53–2.50 (m, 2H), 1.70–1.49 (m, 8H), 1.49–1.39 (m, 10H), 1.31–1.17 (m, 2H). ^{13}C NMR δ 155.4 (C), 134.9 (C), 134.4 (C), 128.8 (CH), 126.7 (CH), 126.2 (CH), 125.7 (CH), 79.0 (C), 56.5 (CH_2), 56.4 (CH_2), 51.2 (CH_2), 46.8 (CH), 34.2 (CH), 32.9 (CH_2), 29.8 (CH_2), 29.2 (CH_2), 28.6 (CH_3), 28.2 (CH_2). HPLC t_R = 8.58 min, >99% purity. HRMS (*m/z*): $[MH]^+$ calcd. for $C_{22}H_{34}N_2O_2$, 359.2693; found 359.2699.

tert-Butyl *(4-(2-(3,4-dihydroisoquinolin-2(1*H*)-yl)ethyl)phenyl)carbamate* (**46**). Using **22** (100 mg, 425 μmol) as the aldehyde, and **23** (68 mg, 510 μmol) as the amine following General Procedure C. Purification by flash column chromatography (petroleum spirits/EtOAc, 1:1) gave the title compound as a pale yellow oil (112 mg, 75%). ^{1}H NMR δ 7.31–7.23 (m, 2H), 7.18–7.07 (m, 5H), 7.05–7.00 (m, 1H), 6.55 (br s, 1H), 3.71 (s, 2H), 2.97–2.68 (m, 8H), 1.51 (s, 9H). ^{13}C NMR δ 153.0 (C), 136.5 (C), 135.1 (C), 134.7 (C), 134.3 (C), 129.3 (CH), 128.8 (CH), 126.7 (CH), 126.2 (CH), 125.7 (CH), 118.9 (CH), 80.5 (C), 60.4 (CH_2), 56.1 (CH_2), 51.1 (CH_2), 33.3 (CH_2), 29.1 (CH_2), 28.5 (CH_3). HPLC t_R = 8.76 min, 95% purity. HRMS (*m/z*): $[MH]^+$ calcd. for $C_{22}H_{28}N_2O_2$, 353.2224; found 353.2220.

tert-*Butyl(*trans-*4-((4-(2,3-dichlorophenyl)piperazin-1-yl)methyl)cyclohexyl)carbamate* (**47**). Using **17** (43 mg, 189 μmol) as the aldehyde, and **28** (48 mg, 208 μmol) as the amine following General Procedure C. Purification by flash column chromatography (petroleum spirits/EtOAc, 1:1) gave the title compound as a pale yellow oil (35 mg, 42%). ^{1}H NMR δ 7.19–7.10 (m, 2H), 6.99–6.92 (m, 1H), 4.39 (br s, 1H), 3.40 (br s, 1H), 3.08 (br s, 4H), 2.61 (br s, 4H), 2.24 (d, *J* = 5.7 Hz, 2H), 2.06–1.99 (m, 2H), 1.91–1.84 (m, 2H), 1.44 (s, 9H), 1.16–0.93 (m, 4H). ^{13}C NMR δ 155.4 (C), 151.4 (C), 134.1 (C), 127.6 (C, CH), 124.7 (CH), 118.7 (CH), 79.2 (C), 65.0 (CH_2), 53.9 (CH_2), 51.3 (CH_2), 50.2 (CH), 34.4 (CH), 33.4 (CH_2),

30.6 (CH_2), 28.6 (CH_3). HPLC t_R = 9.50 min, >99% purity. HRMS (*m/z*): $[MH]^+$ calcd. for $C_{22}H_{33}Cl_2N_3O_2$, 442.2023; found 442.2037.

tert-*Butyl ((*trans-*4((4-(2,3dichlorophenyl)piperazin-1-yl)methyl)cyclohexyl)methyl)carbamate* (**48**). Using **18** (230 mg, 953 µmol) as the aldehyde and **28** (264 mg, 1.14 mmol) as the amine following General Procedure C. Purification by flash column chromatography (petroleum spirits/EtOAc, 3:1) gave the title compound as white needles (198 mg, 46%). mp: 115-116 °C. ^{1}H NMR δ 7.18–7.09 (m, 2H), 6.99–6.91 (m, 1H), 4.59 (br s, 1H), 3.05 (br s, 4H), 2.98 (app t, *J* = 6.1 Hz, 2H), 2.58 (br s, 4H), 2.21 (d, *J* = 7.0 Hz, 2H), 1.94–1.71 (m, 4H), 1.46–1.38 (s, 11H), 1.01–0.83 (m, 4H). ^{13}C NMR δ 156.2 (C), 151.6 (C), 134.1 (C), 127.5 (C, CH), 124.6 (CH), 118.7 (CH), 79.2 (C), 65.6 (CH_2), 53.9 (CH_2), 51.5 (CH_2), 47.0 (CH_2), 38.8 (CH), 35.2 (CH), 31.4 (CH_2), 30.5 (CH_2), 28.6 (CH_3). HPLC t_R = 9.82 min, >99% purity. HRMS (*m/z*): $[MH]^+$ calcd. for $C_{23}H_{35}Cl_2N_3O_2$, 456.2179; found 456.2191.

tert-*Butyl (*cis-*4-(2-(4-(2,3-dichlorophenyl)piperazin-1-yl)ethyl)cyclohexyl)carbamate* (**49**). Using **19** (170 mg, 704 µmol) as the aldehyde, and **28** (195 mg, 845 µmol) as the amine following General Procedure C. Purification by flash column chromatography (petroleum spirits/EtOAc, 3:1) gave the title compound as a colourless oil that foamed under vacuum (256 mg, 80%). ^{1}H NMR δ 7.18–7.10 (m, 2H), 7.00–6.92 (m, 1H), 4.62 (s, 1H), 3.71 (br s, 1H), 3.07 (br s, 4H), 2.63 (br s, 4H), 2.48–2.37 (m, 2H), 1.71–1.53 (m, 6H), 1.53–1.37 (m, 12H), 1.30–1.15 (m, 2H). ^{13}C NMR δ 155.4 (C), 151.5 (C), 134.2 (C), 127.7 (C), 127.6 (CH), 124.7 (CH), 118.7 (CH), 79.2 (C), 56.8 (CH_2), 53.6 (CH_2), 51.5 (CH_2), 46.8 (CH), 34.3 (CH), 32.6 (CH_2), 29.8 (CH_2), 28.6 (CH_3), 28.2 (CH_2). HPLC t_R = 9.96 min, >99% purity. HRMS (*m/z*): $[MH]^+$ calcd. for $C_{23}H_{35}Cl_2N_3O_2$, 456.2179; found 456.2201.

trans-*4-(2-(4-(2,3-Dichlorophenyl)piperazin-1-yl)ethyl)cyclohexanamine* (**50**).[51] Starting with **32**, following General Procedure D, gave the title compound as a pale yellow wax

(99%). ^{1}H NMR δ 7.19–7.09 (m, 2H), 6.99–6.92 (m, 1H), 3.07 (br s, 4H), 2.74–2.55 (m, 5H), 2.48–2.36 (m, 2H), 1.92–1.81 (m, 2H), 1.81–1.72 (m, 2H), 1.50–1.32 (m, 4H), 1.30–1.16 (m, 1H), 1.15–0.92 (m, 4H). ^{13}C NMR δ 151.5 (C), 134.2 (C), 127.6 (C), 127.6 (CH), 124.6 (CH), 118.7 (CH), 56.9 (CH_2), 53.6 (CH_2), 51.5 (CH_2), 50.9 (CH), 36.9 (CH_2), 35.7 (CH), 34.2 (CH_2), 32.3 (CH_2).

cis-*4-(2-(3,4-Dihydroisoquinolin-2(1*H*)-yl)ethyl)cyclohexanamine* (**51**). Starting with **45**, following General Procedure D gave the title compound as an orange oil (87%). ^{1}H NMR δ 7.14–7.06 (m, 3H), 7.04–6.98 (m, 1H), 3.62 (s, 2H), 2.99–2.87 (m, 3H), 2.72 (t, J = 5.9 Hz, 2H), 2.57–2.46 (m, 2H), 1.65–1.39 (m, 11H), 1.27 (br s, 2H). ^{13}C NMR δ 135.1 (C), 134.5 (C), 128.8 (CH), 126.7 (CH), 126.2 (CH), 125.7 (CH), 56.8 (CH_2), 56.5 (CH_2), 51.2 (CH_2), 47.9 (CH), 33.8 (CH), 32.6 (CH_2), 32.2 (CH_2), 29.3 (CH_2), 27.9 (CH_2).

*(*trans-*4-((4-(2,3-Dichlorophenyl)piperazin-1-yl)methyl)cyclohexyl)methanamine* (**52**). Starting with **48**, following General Procedure D, gave the title compoud as a white wax (90%). ^{1}H NMR δ 7.17–7.09 (m, 2H), 7.00–6.90 (m, 1H), 3.06 (br s, 4H), 2.67–2.49 (m, 6H), 2.22 (d, J = 7.1 Hz, 2H), 1.95–1.75 (m, 4H), 1.49 (br s, 1H), 1.35–1.10 (m, 3H), 0.99–0.82 (m, 4H). ^{13}C NMR δ 151.6 (C), 134.1 (C), 127.6 (C), 127.5 (CH), 124.6 (CH), 118.7 (CH), 65.8 (CH_2), 53.9 (CH_2), 51.5 (CH_2), 49.0 (CH_2), 41.8 (CH), 35.5 (CH), 31.6 (CH_2), 30.6 (CH_2). HPLC (λ = 214 nm) t_R = 7.13 min, >99 % purity.

cis-*4-(2-(4-(2,3-Dichlorophenyl)piperazin-1-yl)ethyl)cyclohexanamine* (**53**). Starting with **49**, following General Procedure D, gave the title compound as a pale yellow oil (81%). ^{1}H NMR δ 7.19–7.09 (m, 2H), 7.01–6.91 (m, 1H), 3.08 (br s, 4H), 3.00–2.88 (m, 1H), 2.64 (br s, 4H), 2.46–2.37 (m, 2H), 1.65–1.25 (m, 13H). ^{13}C NMR δ 151.5 (C), 134.1 (C), 127.63 (C), 127.56 (CH), 124.6 (CH), 118.7 (CH), 57.1 (CH_2), 53.6 (CH_2), 51.5 (CH_2), 47.8 (CH), 34.0 (CH), 32.6 (CH_2), 31.9 (CH_2), 27.9 (CH_2).

General Procedure F (*N*,*N*-Dimethylurea Synthesis)

The amine starting material was taken in DCM (5 mL) and Et_3N at RT under N_2. To the stirred solution was slowly added dimethylcarbamyl chloride (TOXIC, 2 equiv), and after 18 h, was diluted with DCM (20 mL) and washed with 1% NH_4OH solution (2 × 15 mL), brine (10 mL), then dried over anhydrous Na_2SO_4 and evaporated to dryness. The material was then purified by flash column chromatography.

*3-(*trans*-4-(2-(4-(2,3-Dichlorophenyl)piperazin-1-yl)ethyl)cyclohexyl)-1,1-dimethylurea* (**2**).[12] Following General procedure F, using **50** (40 mg, 112 μmol) as the amine, the product was eluted ($CHCl_3$/CH_3OH, 20:1 to 10:1) to give the title compound as a white solid (27 mg, 56%). mp: 208-209 °C. ^{1}H NMR δ 7.18–7.10 (m, 2H), 6.99–6.92 (m, 1H), 4.12 (d, J = 7.5 Hz, 1H), 3.64–3.49 (m, 1H), 3.07 (br s, 4H), 2.88 (s, 6H), 2.63 (br s, 4H), 2.50–2.39 (m, 2H), 2.07–1.94 (m, 2H), 1.82–1.72 (m, 2H), 1.52–1.37 (m, 2H), 1.31–1.18 (m, 1H), 1.18–0.99 (m, 4H). ^{13}C NMR δ 157.8 (C), 151.3 (C), 134.0 (C), 127.5 (C), 127.4 (CH), 124.5 (CH), 118.6 (CH), 56.7 (CH_2), 53.4 (CH_2), 51.3 (CH_2), 49.8 (CH), 36.1 (CH_3), 35.7 (CH), 34.0 (CH_2), 33.9 (CH_2), 32.1 (CH_2). HPLC t_R = 8.60 min, >99% purity. HRMS (*m/z*): $[MH]^+$ calcd. for $C_{21}H_{32}Cl_2N_4O$, 427.2026; found 427.2022.

*3-(*cis*-4-(2-(3,4-Dihydroisoquinolin-2(1*H*)-yl)ethyl)cyclohexyl)-1,1-dimethylurea* (**54**). Following General procedure F, using **51** (40 mg, 155 μmol) as the amine, the product was eluted ($CHCl_3$/CH_3OH, 50:1 to 20:1) to give the title compound as a pale yellow wax (17 mg, 33%). ^{1}H NMR δ 7.17–7.06 (m, 3H), 7.05–6.97 (m, 1H), 4.39 (d, J = 6.7 Hz, 1H), 3.90 (br s, 1H), 3.62 (s, 2H), 2.96–2.86 (m, 8H), 2.73 (t, J = 5.9 Hz, 2H), 2.57–2.45 (m, 2H), 1.70–1.44 (m, 9H), 1.32–1.18 (m, 2H). ^{13}C NMR δ 157.9 (C), 135.0 (C), 134.5 (C), 128.8 (CH), 126.7 (CH), 126.2 (CH), 125.7 (CH), 56.6 (CH_2), 56.5 (CH_2), 51.2 (CH_2), 46.8 (CH), 36.3 (CH_3), 34.0 (CH), 32.8 (CH_2), 30.1 (CH_2), 29.3 (CH_2), 28.5 (CH_2). HPLC t_R = 7.13 min, 99% purity. HRMS (*m/z*): $[MH]^+$ calcd. for $C_{20}H_{31}N_3O$, 330.2540; found 330.2538.

*3-((*trans-*4-((4-(2,3-Dichlorophenyl)piperazin-1-yl)methyl)cyclohexyl)methyl)-1,1-dimethylurea* (**55**). Following General procedure F, using **52** (40 mg, 112 µmol) as the amine, the product was eluted ($CHCl_3/CH_3OH$, 5:1) to give the title compound as a colourless oil (32 mg, 67%). ^{1}H NMR δ 7.17–7.09 (m, 2H), 6.98–6.92 (m, 1H), 4.45 (br s, 1H), 3.13–3.00 (m, 6H), 2.90 (s, 6H), 2.58 (br s, 4H), 2.21 (d, J = 7.0 Hz, 2H), 1.83 (m, 4H), 1.57–1.38 (m, 2H), 1.00–0.84 (m, 4H). ^{13}C NMR δ 158.7 (C), 151.5 (C), 134.1 (C), 127.6 (C), 127.5 (CH), 124.5 (CH), 118.7 (CH), 65.6 (CH_2), 53.9 (CH_2), 51.4 (CH_2), 47.3 (CH_2), 38.8 (CH), 36.3 (CH_3), 35.3 (CH), 31.4 (CH_2), 30.6 (CH_2). HPLC t_R = 8.83 min, 98% purity. HRMS (*m/z*): $[MH]^+$ calcd. for $C_{21}H_{32}Cl_2N_4O$, 427.2026; found 427.2045.

*3-(*cis-*4-(2-(4-(2,3-Dichlorophenyl)piperazin-1-yl)ethyl)cyclohexyl)-1,1-dimethylurea* (**56**). Following General procedure F, using **53** (40 mg, 112 µmol) as the amine, the product was eluted ($CHCl_3/CH_3OH$, 50:1 to 20:1) to give the title compound as a pale yellow solid (17 mg, 33%). mp: 174-175 °C. ^{1}H NMR δ 7.19–7.10 (m, 2H), 6.99–6.93 (m, 1H), 4.38 (d, J = 6.9 Hz, 1H), 3.95–3.80 (m, 1H), 3.08 (br s, 4H), 2.90 (s, 6H), 2.65 (br s, 4H), 2.50–2.38 (m, 2H), 1.70–1.40 (m, 9H), 1.31–1.16 (m, 2H). ^{13}C NMR δ 157.9 (C), 151.4 (C), 134.2 (C), 127.50 (C), 127.45 (CH), 124.7 (CH), 118.7 (CH), 56.8 (CH_2), 53.6 (CH_2), 51.5 (CH_2), 46.8 (CH), 36.3 (CH_3), 34.0 (CH), 32.4 (CH_2), 30.1 (CH_2), 28.5 (CH_2). HPLC t_R = 8.93 min, >99 % purity. HRMS (*m/z*): $[MH]^+$ calcd. for $C_{21}H_{32}Cl_2N_4O$, 427.2026; found 427.2025.

Biological Assays

Cell Lines and Transfection

FlpIn CHO cells (Invitrogen, Carlsbad, USA) were grown in Dulbecco's modified Eagle's medium (DMEM) supplemented with 10% fetal bovine serum and maintained at 37 °C in a

humidified incubator containing 5% CO_2. The FlpIn CHO cells were transfected with the pOG44 vector encoding Flp recombinase and the pDEST vector encoding the wild-type long isoform of the human D_2 receptor ($D_{2L}R$) at a ratio of 9:1 using polyethylenimine as transfection reagent.[52] 24 h after transfection the cells were subcultured and the medium was supplemented with 700µg/ml HygroGold as selection agent. Cells were grown and maintained in DMEM containing 20 mM HEPES, 5% fetal bovine serum and 200 µg/mL Hygromycin-B. Cells were maintained at 37 °C in a humidified incubator containing 5% CO_2, 95% O_2.

Preparation of FlpIN CHO cell membranes

When cells were approximately 90% confluent, they were harvested and centrifuged (300 g, 3 min). The resulting pellet was resuspended in assay buffer (20 mM HEPES, 100 mM NaCl, 6 mM $MgCl_2$, 1 mM EGTA, 1 mM EDTA; pH 7.4), and the centrifugation procedure repeated. The intact cell pellet was then resuspended in assay buffer and homogenised using a Polytron homogeniser for three 10-second intervals on the maximum setting, with 30-second periods on ice between each burst. The homogenate was made up to 30 mL and centrifuged (1,000 g, 10 min, 25 °C), the pellet discarded and the supernatant recentrifuged at 30,000 g for 1 h at 4 °C. The resulting pellet was resuspended in 5 mL assay buffer and the protein content determined using the method of Bradford. The homogenate was then separated into 1 mL aliquots and stored frozen at -80 °C until required for binding assays.

[^{3}H]spiperone binding assay

Cell membranes (D_{2L}-Flp-In CHO, 3 µg) were incubated with varying concentrations of test compound in binding buffer (20 mM HEPES, 100 mM NaCl, 6 mM $MgCl_2$, 1 mM EGTA, 1 mM EDTA; pH 7.4) containing 0.05 nM of [^{3}H] spiperone and 100 µM GppNHp to a final

volume of 1 mL and incubated at 37 °C for 3 h. Binding was terminated by fast flow filtration over GF/B membranes using a brandel harvester followed by three washes with ice-cold 0.9% NaCl. Bound radioactivity was measured in a Tri-Carb 2900TR liquid scintillation counter (Perkin Elmer).

cAMP Accumulation Assay

cAMP responses were measured using an Alphascreen cAMP accumulation assay (PerkinElmer, Waltham, USA). FlpIn CHO cells stably expressing the $D_{2L}R$ were grown overnight in 96-well plates at a density of 50,000 cells/well. After pre-incubating the cells for 45 min with stimulation buffer (Hank's buffered salt solution: 0.14 M NaCl, 5.4 mM KCl, 0.8 μM $MgSO_4$, 1.3 mM $CaCl_2$, 0.2 mM Na_2HPO_4, 0.44 mM KH_2PO_4, 5.6 mM D-glucose, 1mg/ml BSA, 0.5mM 3-isobutyl-1-methylxanthine, and 5 mM HEPES, pH 7.4) the cells were stimulated simultaneously with drug and 300 nM forskolin for 30 min at 37 °C. Stimulation of cells was terminated by the removal of the stimulation buffer and the addition of 50 μl ice-cold 100% EtOH. The plates containing the cell lysates were then incubated at 37 °C without lid to allow complete evaporation of the EtOH. After all the EtOH was evaporated, 50 μl of detection buffer (1 mg/ml BSA, 0.3% Tween-20, and 5mM HEPES, pH 7.4) was added to each well. The plate was shaken for 5 min and the bottom of the wells were scraped to ensure complete and even suspension of the cell material. 5 μl of the samples was then transferred into a white 384-well Optiplate (PerkinElmer, Waltham, USA). Anti-cAMP acceptor beads (0.2 units/μl) diluted in stimulation buffer were added to all samples and incubated in the dark at room temperature for 30 min before addition of 15 μl of the donor beads/biotinylated cAMP (0.07 units/ul) mixture made up in detection buffer. Following a 1 h incubation at RT, plates were read using a Fusion-TM plate reader (PerkinElmer, Waltham, USA).

ERK1/2 Phosphorylation Assay

FlpIn CHO cells stably expressing the $D_{2L}R$ were seeded into 96-well plates at a density of 50,000 cells/well. After 5-7 h, cells were washed with phosphate-buffered saline (PBS) and incubated in serum-free DMEM overnight before assaying. Initially, time-course experiments were conducted at least twice for each ligand to determine the time required to maximally promote ERK1/2 phosphorylation via the dopamine $D_{2L}R$. Dose-response experiments were performed in the absence and presence of increasing concentrations of each ligand at 37 °C. Stimulation of the cells was terminated by removing the media and the addition of 100 µl of SureFire lysis buffer (PerkinElmer, Waltham, USA) to each well. The plate was shaken for 5 min at RT before transferring 5 µl of the lysates to a white 384-well Proxiplate (PerkinElmer, Waltham, USA). Then 8 µl of a 240:1440:7:7 mixture of Surefire activation buffer : Surefire reaction buffer : Alphascreen acceptor beads : Alphascreen donor beads was added to the samples and incubated in the dark at 37 °C for 1.5 h. Plates were read using a Fusion-TM plate reader (PerkinElmer, Waltham, USA).

Molecular Modeling

The generalized numbering scheme proposed by Ballesteros and Weinstein[53] was used for residues in the TM regions of the GPCR.

The sequence of the human dopamine D_2R was retrieved from the Swiss-Prot database. ClustalX software[54] was used to align the sequence with the crystal structure of the human D_3R (PDB ID: 3PBL[55]). The structural model of the receptor was built using the Modeller v9.12 suite of programs,[56] which yielded 10 candidate models. The conserved disulphide bond between residue C3.25 (107) at the beginning of TM3 and the cysteine in the middle of the ECL2 as well as the one between C6.61 (223) and C7.29 (225) in ECL3 present in the template structure were also built and maintained as a constraint for geometric optimization.

The best structure was selected from these candidates, according to the Modeller DOPE assessment score and visual inspection. The resulting receptor structure was optimized using the Duan force field[57] and the general Amber force field (GAFF) and HF/6-31G*-derived RESP atomic charges were used for the ligands[58]

The docking of the compounds was performed with the Molecular Operating Environment of docking (MOE, Chemical Computing Group, Inc). The compounds were docked into the receptor model with their protonated nitrogen interacting with Asp3.32 and their phenyl piperazine or tetrahysroisoquinoline core groups situated within TM3, TM5 and TM6. The obtained complexes were subjected to refinement using MOE in a 200 ps molecular dynamics simulations (force field MMF94x, 300 K, Born solvation, time step 2 fs). Further optimization of the complexes was performed by MD simulation over 200 ps in which the ligands, the binding site (10Å around the ligands) and the ECL2 were kept flexible while protein backbone atoms were kept fixed (MMFF94 force field, Born solvation, 300 K, time step 2fs). The final complex was subsequently energy minimized by applying gradient minimization until the RMS gradient was lower than 0.001 kcal/molÅ. The final complexes were embedded in a pre-equilibrated lipid bilayer (~280 molecules of POPC; ~215000 water molecules and counterions). Simulations were carried out using NAMD2.9[59] package using the TIP3 water model and the CHARMM27 all-hydrogen force field for protein and lipids, using the particle mesh Ewald (PME) method[60] to evaluate electrostaic interactions. After an equilibration period of 1 ns (where we applied a positional restraint of 10 kcal mol^{-1} $Å^{-2}$ to the Cα of the receptor structure) the MD simulations were performed during 20 ns using a 1 fs integration time step, constant pressure and constant temperature of 300 K.

Data Analysis

Agonist dose-response curves were fitted empirically to a three-parameter logistic equation using Prism 6.0 (GraphPad Software Inc., San Diego, CA),

$$Y = bottom + \frac{top - bottom}{1 + 10^{(\log EC_{50} - \log[A])}} \quad (1)$$

where bottom and top are the lower and upper plateaus, respectively, of the concentration-response curve, [A] is the molar concentration of agonist, and EC_{50} is the molar concentration of agonist required to generate a response halfway between the top and the bottom. To compare agonist profiles and quantify stimulus bias, agonist concentration-response data were fitted to the following form of the operational model of agonism;[21]

$$Y = basal + \frac{(E_m - basal)\left(\frac{\tau}{K_A}\right)^n [A]^n}{[A]^n \left(\frac{\tau}{K_A}\right)^n + \left(1 + \frac{[A]}{K_A}\right)^n} \quad (2)$$

where E_m is the maximal possible response of the system; basal is the basal level of response; K_A denotes the equilibrium dissociation constant of the agonist (A); τ is an index of the signalling efficacy of the agonist and is defined as R_T/K_E, where R_T is the total number of receptors and K_E is the coupling efficiency of each agonist-occupied receptor; and n is the slope of the transducer function that links occupancy to response. The analysis assumes that the maximal system responsiveness (E_m) and the transduction machinery utilized for a given cellular pathway are the same for all agonists, such that the E_m and transducer slope (n) are shared between agonists. Data for all compounds for each pathway were fit globally to determine values of K_A and τ.

The ratio, τ/K_A was determined as a logarithm i.e. $\log(\tau/K_A)$ and is referred to herein as the 'transduction coefficient', as this composite parameter is sufficient to describe agonism and bias for a given pathway, i.e. biased agonism can result from either a selective affinity (K_A) of an agonist for a given receptor state(s) and/or a differential coupling efficacy (τ) toward certain pathways.

To cancel the impact of cell-dependent effects on the observed agonism at each pathway, the $\log(\tau/K_A)$ values were then normalized to that determined for the endogenous agonist dopamine at each pathway to yield a 'normalized transduction coefficient,' $\Delta\log(\tau/K_A)$ calculated as follows:

$$\Delta\log\left(\frac{\tau}{K_A}\right) = \log\left(\frac{\tau}{K_A}\right)_{\substack{test\\compound}} - \log\left(\frac{\tau}{K_A}\right)_{ACh} \quad (3).$$

Finally, to determine the actual bias of each agonist for different signalling pathways, the $\Delta\log(\tau/K_A)$ values were evaluated statistically between the pathways. The ligand bias of an agonist for one pathway, j1, over another, j2 is given as:

$$\Delta\Delta\log(\tau/K_A)_{j1-j2} = \Delta\log\left(\frac{\tau}{K_A}\right)_{j1} - \Delta\log\left(\frac{\tau}{K_A}\right)_{j2} \quad (4).$$

A lack of biased agonism as compared to the reference agonist dopamine will result in values of $\Delta\Delta\log(\tau/K_A)$ not significantly different from 0 between pathways. To account for the propagation of error associated with the determination of composite parameters using equations 3 & 4, the following equation was used:

$$Pooled\_SEM = \sqrt{(SEj1)^2 + (SEj2)^2} \quad (5).$$

All affinity (pK_i or pK_A), potency (pEC_{50}), efficacy (τ) and transduction ratio ($\Delta\Delta\log(\tau/K_A)$) parameters were estimated as logarithms. When fold-changes in bias, functional affinity or efficacy are described this was calculated by first converting values of $\Delta\Delta\log(\tau/K_A)$, pK_A or $\log\tau$ to the corresponding antilog value. Taking bias as an example:

$$Bias = 10^{\Delta\Delta\log\left(\frac{\tau}{K_A}\right)} \quad (6).$$

However, we and others have previously demonstrated that such the distribution of these parameters does not conform to a normal (Gaussian) distribution whereas the logarithm of the measure is approximately Gaussian.[61-63] Thus, since the application of t tests and analyses of variance assume Gaussian distribution, estimating the parameters as logarithms allows valid statistical comparison. All results are expressed as the mean ± S.E.M. Statistical analyses were performed where appropriate using one-way ANOVA with the Tukey's post-test statistical significance was taken as $p < 0.05$. Where only two values were compared then an unpaired two-tailed Student's t-test was used. It should be noted that both the Student's t-test and ANOVA analyses assume equal variances. In particular when considering values of affinity obtained in different assays such equal variances cannot be assumed. As such we performed a Brown-Forsythe test (Graphpad prism 6) to assure ourselves of equal variance when such parameters are compared.

Scheme 1. Synthesis of spacer groups with variations in spacer length, aromaticity and stereoisomerism.[a]

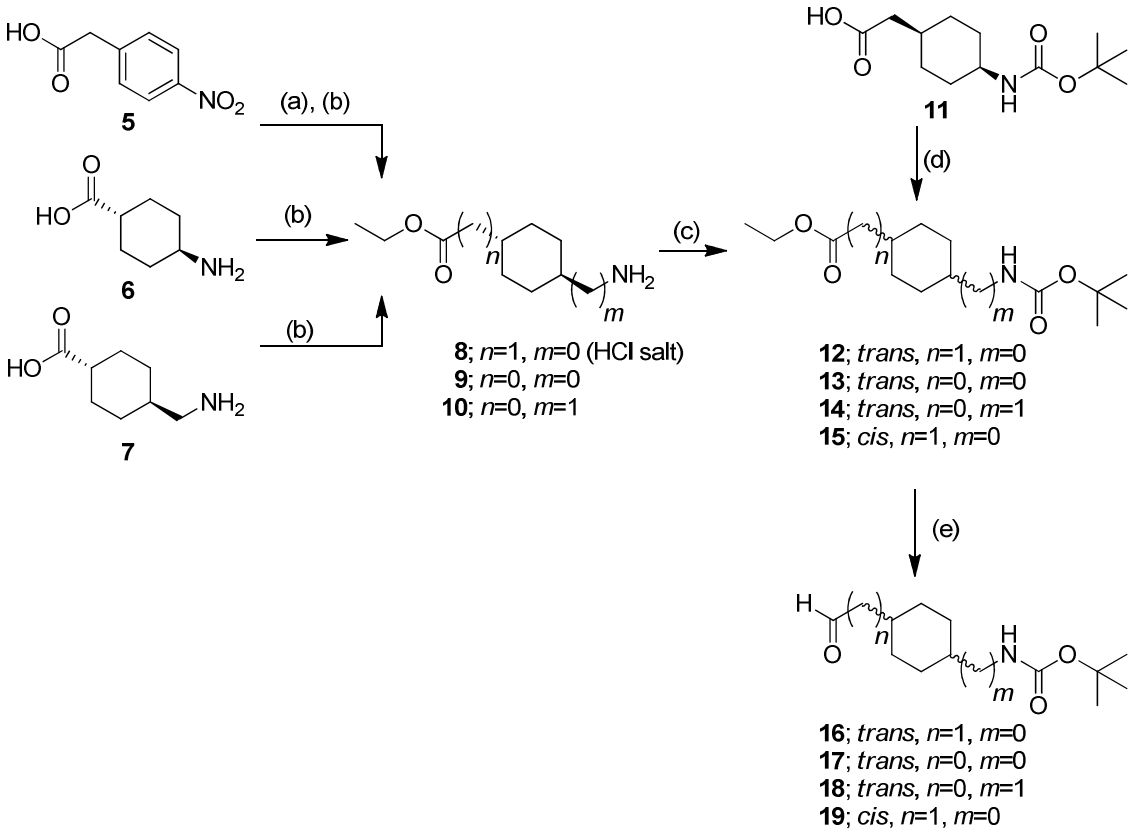

[a]Reagents and conditions: (a) 10% Pd/C, H_2, 60 psi, rt, 3 d (b) EtOH, HCl, reflux, 2-36 h, 66-81%; (c) Boc anhydride, Et_3N, DCM, rt, 2-24 h, 58-96%; (d) EDCI, DMAP, EtOH, rt, 24 h, 64%; (e) DIBALH, toluene, -78 °C, 30 min, 89-99%.

Scheme 2. Synthesis of aromatic spacer.[a]

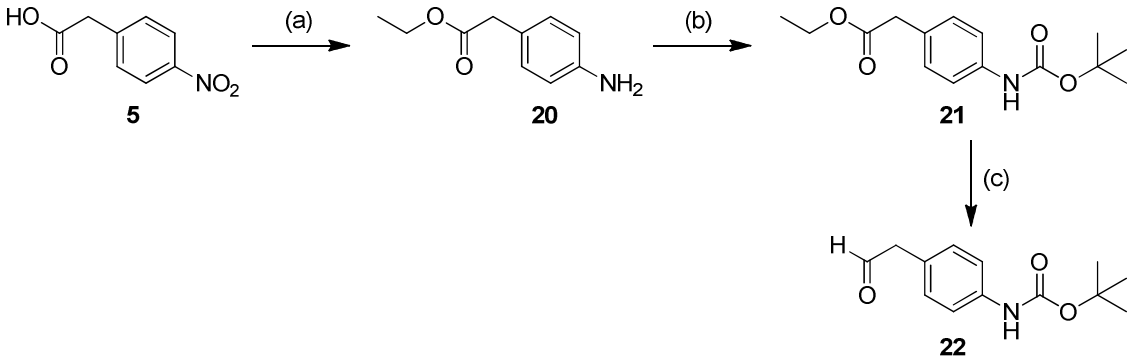

[a]Reagents and conditions: (a) EtOH, HCl, reflux, 2 h, followed by EtOH, Sn, HCl, reflux, 16 h, 77%; (b) Boc anhydride, Et_3N, DCM, rt, 24 h, 76%; (c) DIBAL-H, toluene, -78 °C, 30 min, 99%.

Scheme 3. Synthesis of head groups.[a]

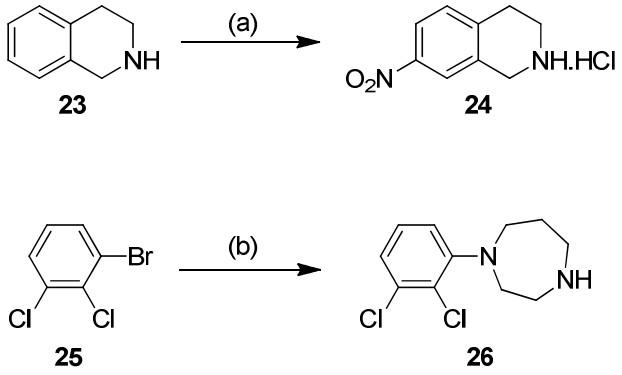

[a]Reagents and conditions: (a) $NaNO_3$, H_2SO_4, 0 °C, 20 h, followed by conc. HCl, 67%; (b) homopiperazine, $Pd_2(dba)_3$, BINAP, *t*-BuOK, BOC_2O, toluene, TFA, 80 °C, 24 h, 3%;

Scheme 4. Synthesis of **4**, and target compounds with variations in head group (**29-32**).[a]

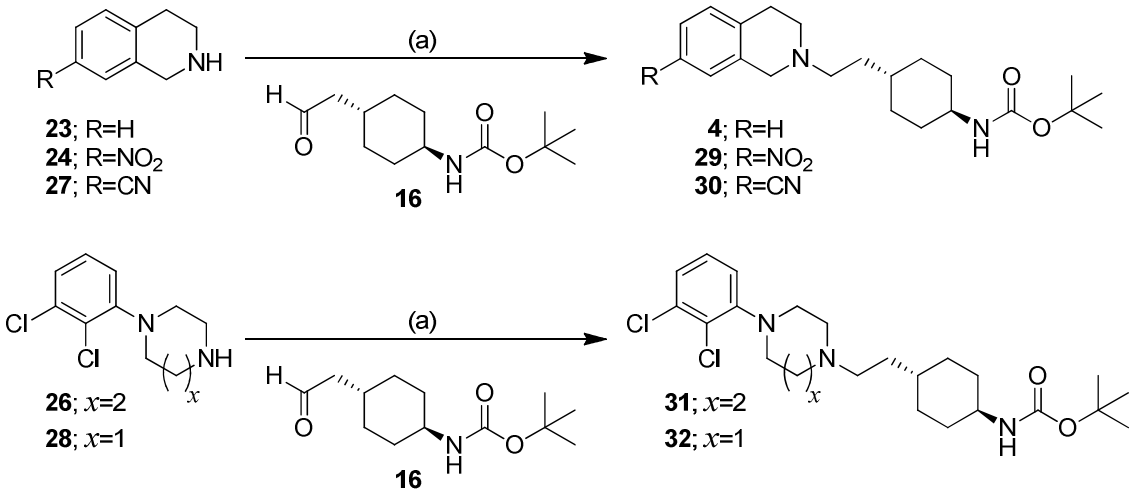

[a]Reagents and conditions: (a) $NaBH(OAc)_3$, 1,2-DCE, rt, 16-24 h, 22-85%.

Scheme 5. Synthesis of target compounds with variations to the tail group based on **4** and **30**.[a]

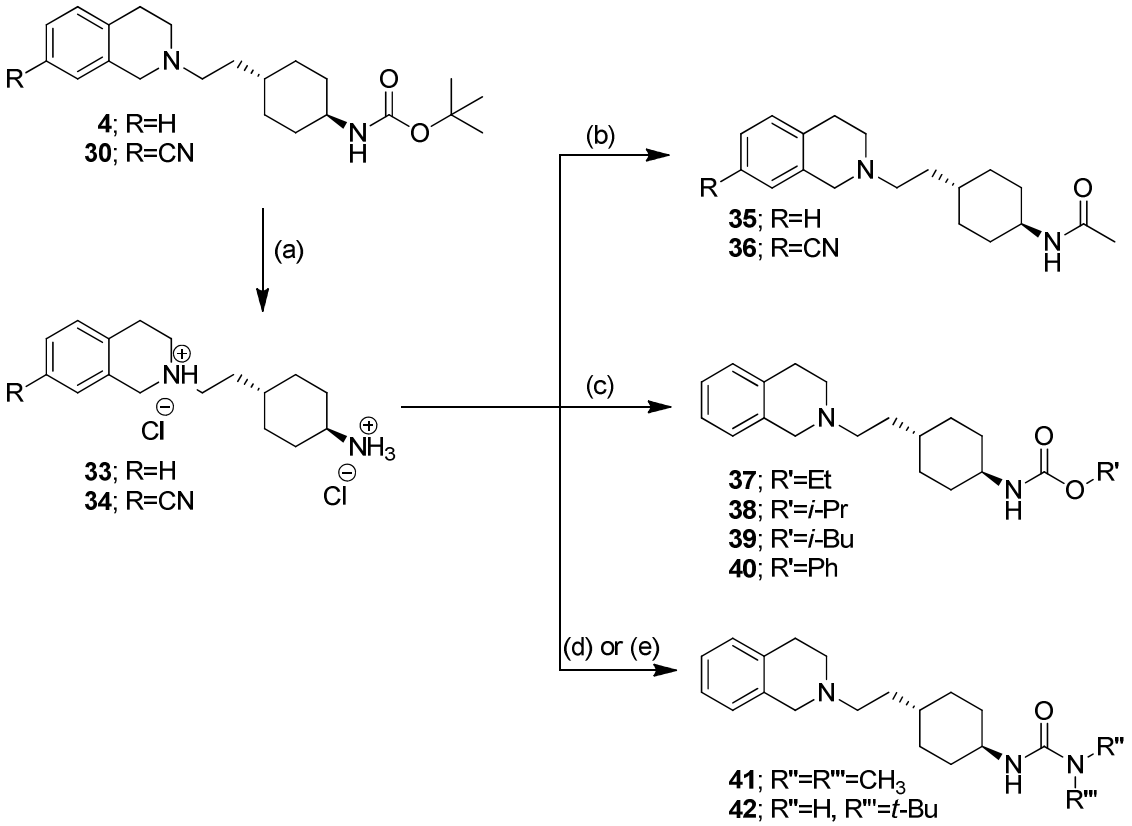

[a]Reagents and conditions: (a) TFA, DCM, rt, 2-24 h, followed by base then 1M HCl in Et_2O, 80-99%; (b) Ac_2O, DIPEA, DCM, rt, 2 h, 26-87%; (c) ethyl pyrocarbonate or *i*-propyl/*i*-butyl/phenyl chloroformate, DCM, TEA, rt, 1-14 h, 49-90%; (d) dimethylcarbamyl chloride, DCM, rt, 24 h, 33-82%; (e) *tert*-butylamine, CDI, TEA, MeCN, rt, 16 h, 43%.

Scheme 6. Synthesis of target compounds (**43-49**) with variations in length and nature of the spacer group for THIQ and 2,3-DCPP head groups.[a]

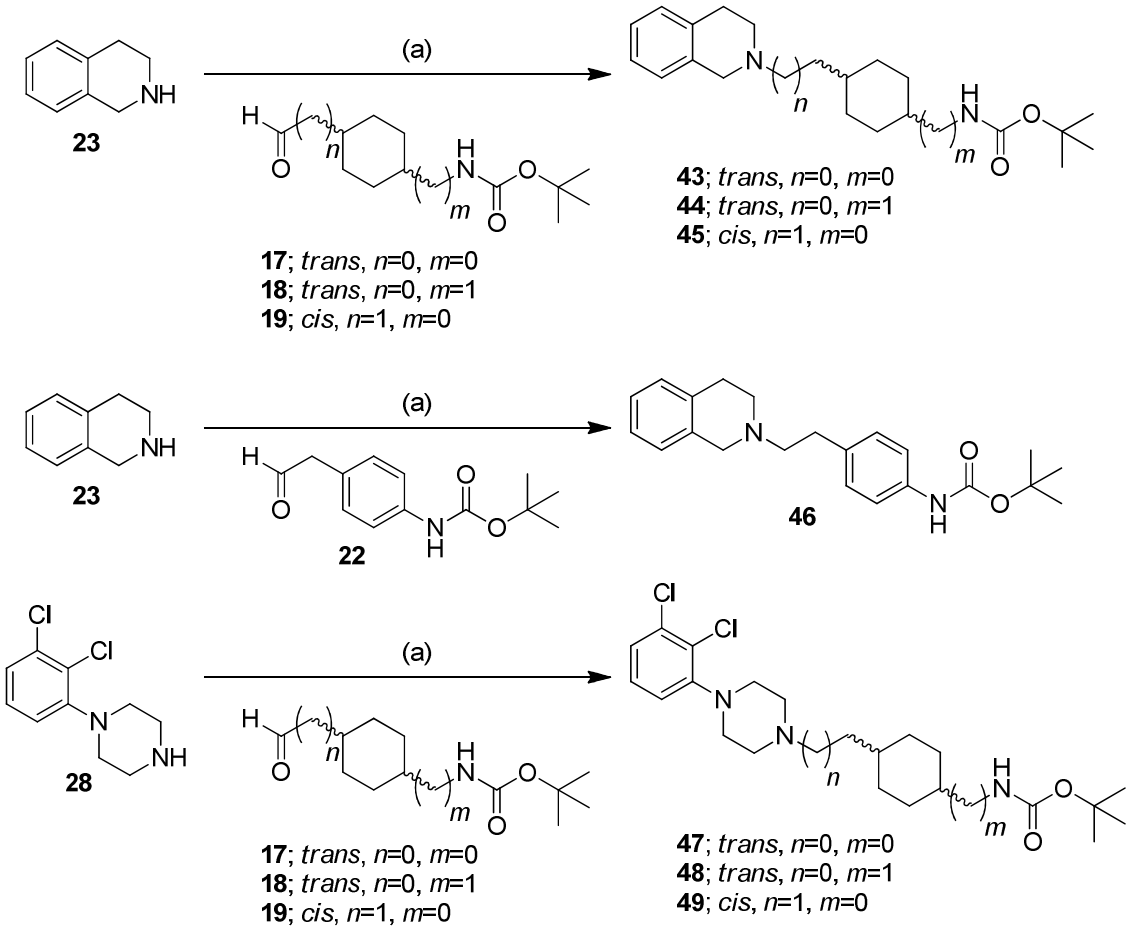

[a]Reagents and conditions: (a) $NaBH(OAc)_3$, 1,2-DCE, rt, 16-24 h, 22-85%.

Scheme 7. Synthesis of compounds with the *N*,*N*-dimethylurea tail group (**3**, **54-56**).[a]

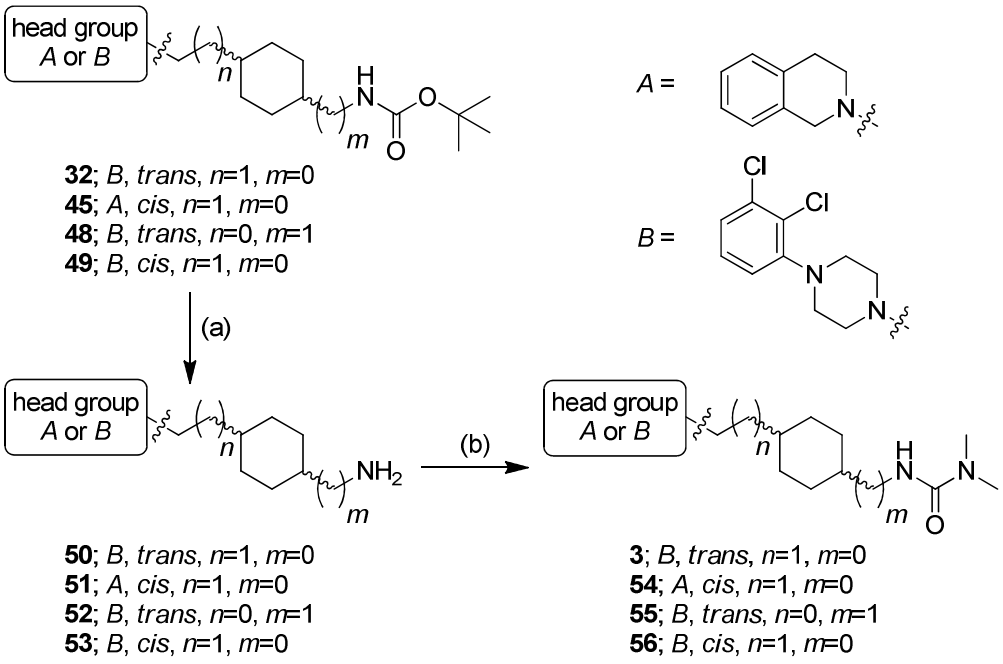

[a]Reagents and conditions: (a) TFA, DCM, rt, 2-24 h, followed by base, 80-99%; (b) dimethylcarbamyl chloride, DCM, rt, 24 h, 33-56%.

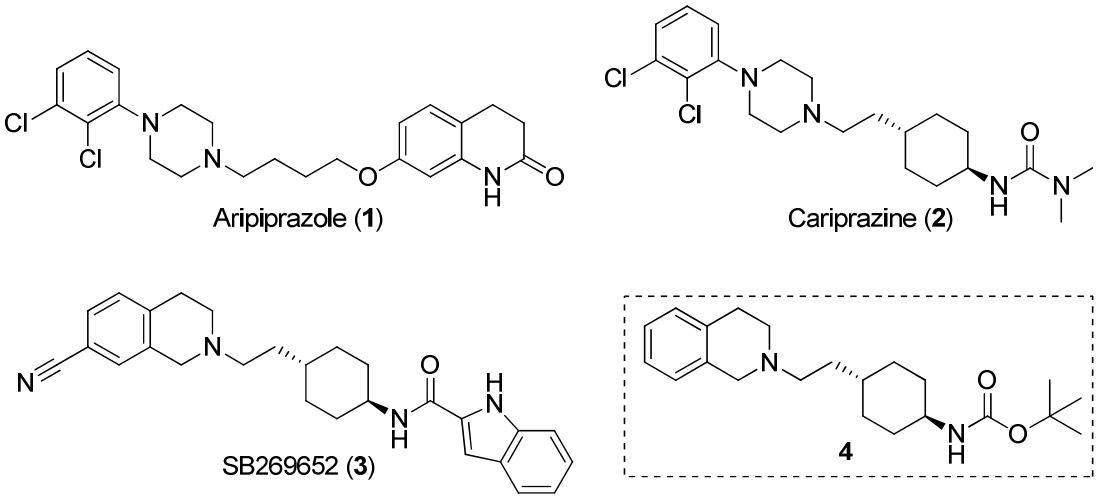

Figure 1: Chemical structures of aripiprazole (**1**), a potent D_2R partial agonist marketed for the treatment of schizophrenia; cariprazine (**2**), a D_2R partial agonist currently awaiting FDA approval for the treatment of schizophrenia and bipolar depression; SB269652 (**3**), a D_3R selective antagonist / D_2R negative allosteric modulator; and, *tert*-butyl (*trans*-4-(2-(3,4-dihydroisoquinolin-2(1*H*)-yl)ethyl)cyclohexyl)carbamate (**4**), the hit compound discovered to be a D_2R partial agonist with sub-micromolar potency.

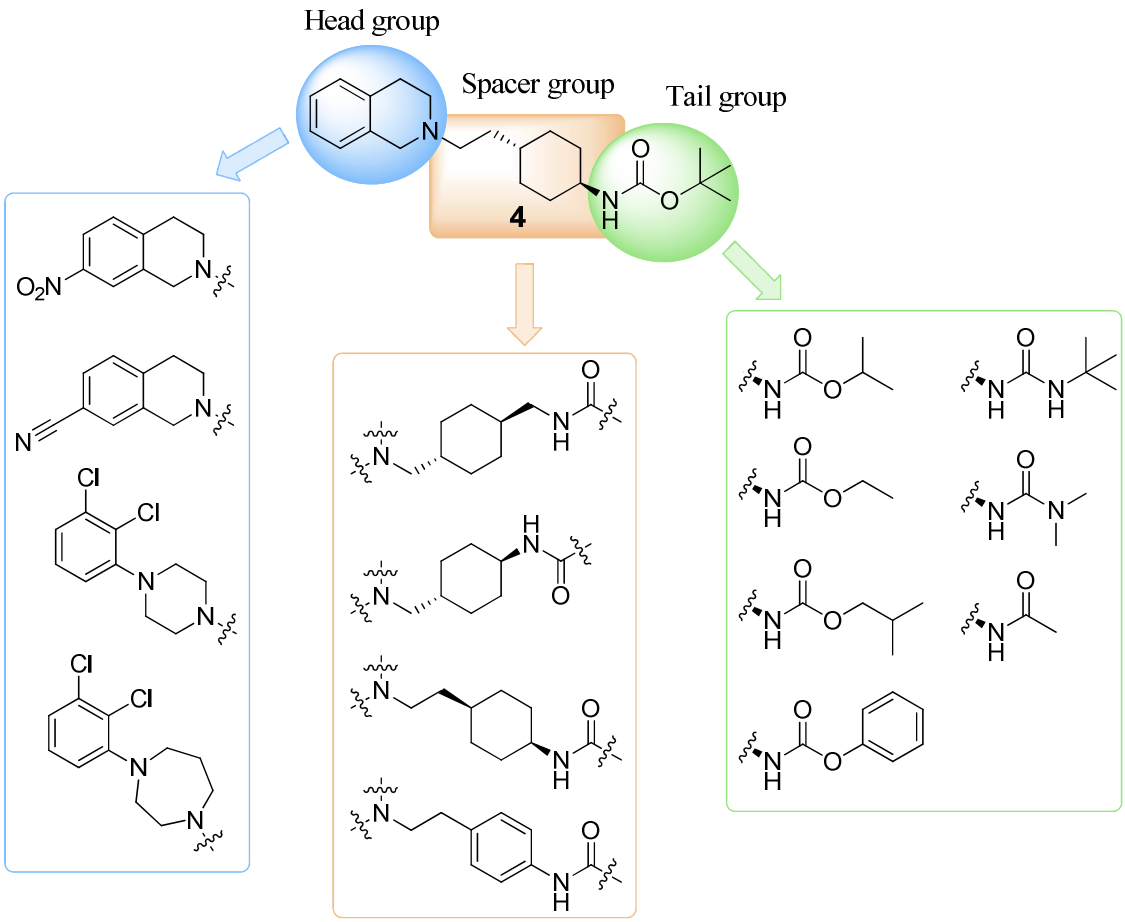

Figure 2: Investigation of SAR for biased agonists based on the scaffold of **4** by exploring three main regions of the lead compound; the tertiary amine-containing head group (blue), the cyclohexylene spacer group (orange), and the *tert*-butyl carbamate tail group (green).

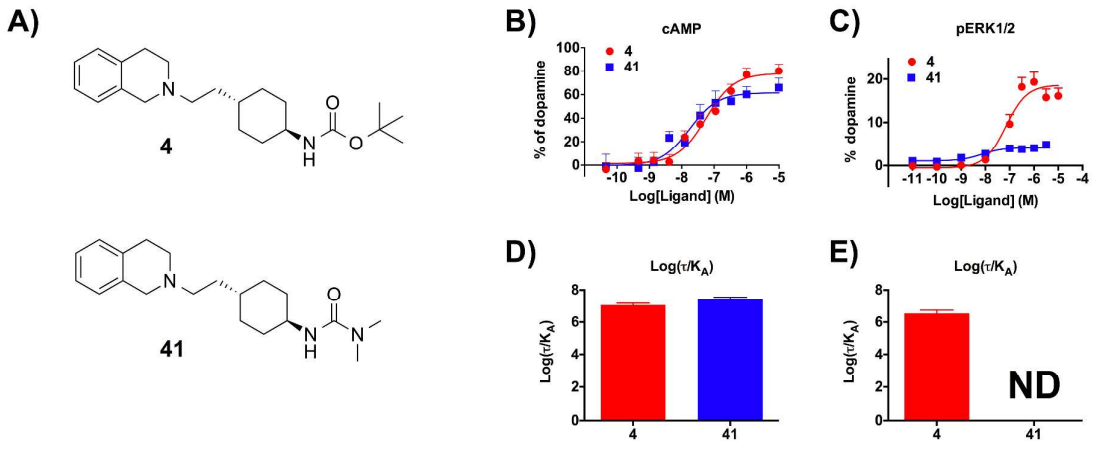

Figure 3: A) Modification of the *tert*-butyl carbamate tail group of **4** to the *N*,*N*-dimethylurea tail group (**41**) maintains activity in an assay measuring inhibition of forskolin stimulated cAMP (B) as quantified using transduction coefficients (D) but causes a complete loss of activity in the pERK1/2 assay (C & E, ND indicates that a transduction coefficient could not be derived). As such, this modification confers biased agonism towards the cAMP pathway.

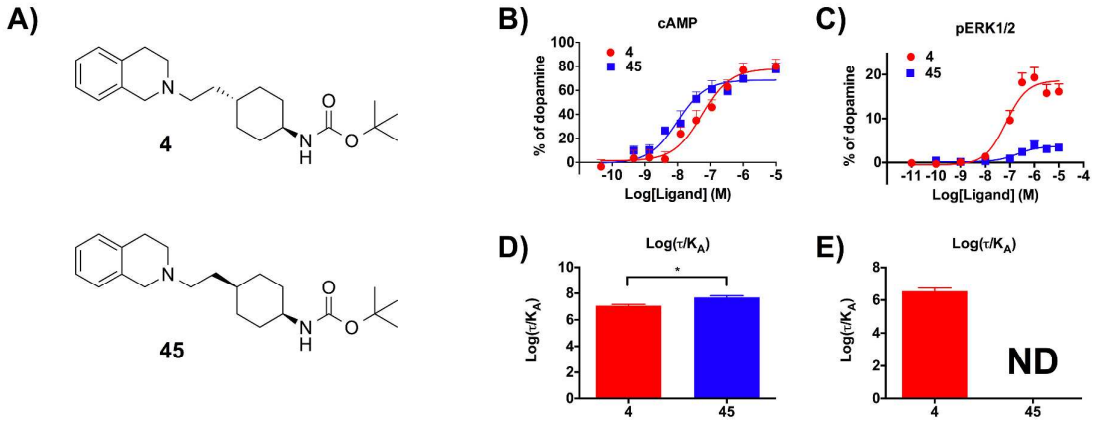

Figure 4: A) Modification of the spacer group from the *trans* (**4**) to the *cis* stereoisomer (**45**) increases activity in an assay measuring inhibition of forskolin-stimulated cAMP (B) as quantified using transduction coefficients (D) but causes a complete loss of agonism in the pERK1/2 assay (C & E, ND indicates that a transduction coefficient could not be derived). As such, this modification confers biased agonism towards the cAMP pathway.

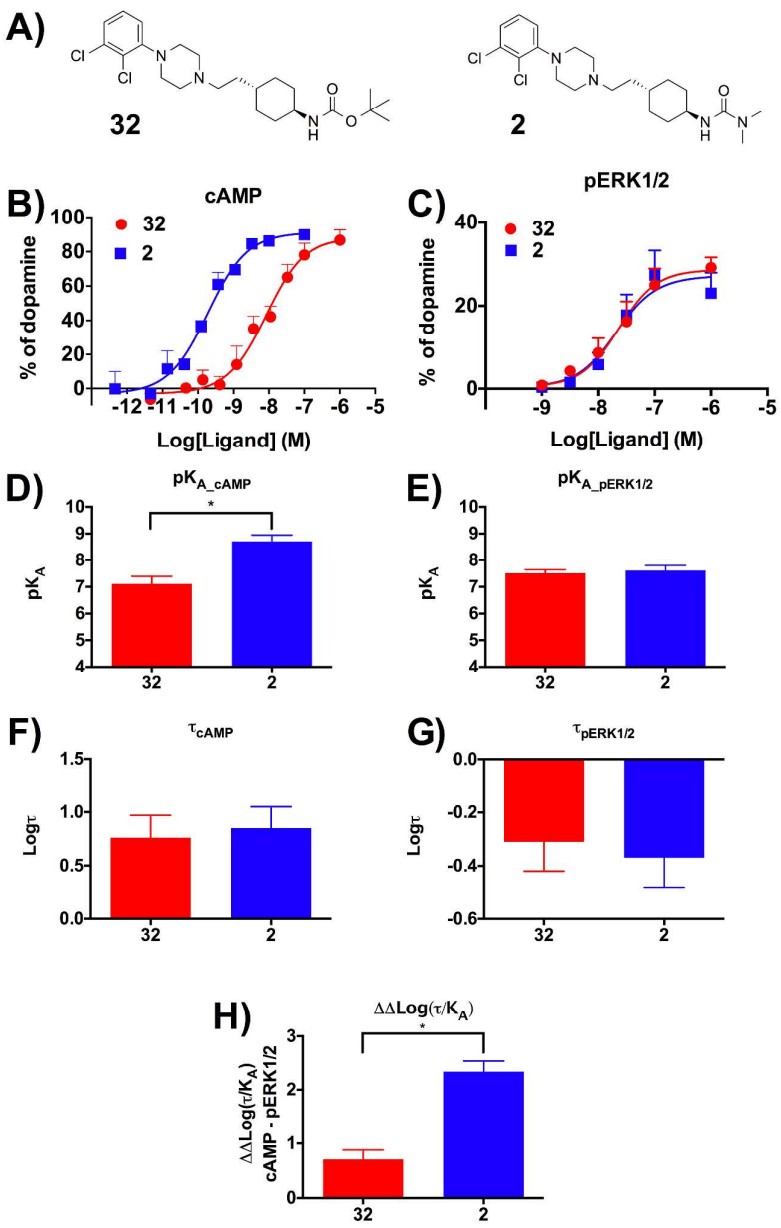

Figure 5: A) Modification of the *tert*-butyl carbamate tail group of **32** to the *N*,*N*-dimethylurea tail group (cariprazine, **2**) increases (B) potency; and (D) functional affinity in an assay measuring inhibition of forskolin stimulated cAMP; but (F) maintains the level of efficacy, τ_{cAMP}. In contrast, this modification caused no significant change in either parameter in the pERK1/2 assay (C, E and G). As such, this modification confers significant biased agonism towards the cAMP pathway (H).

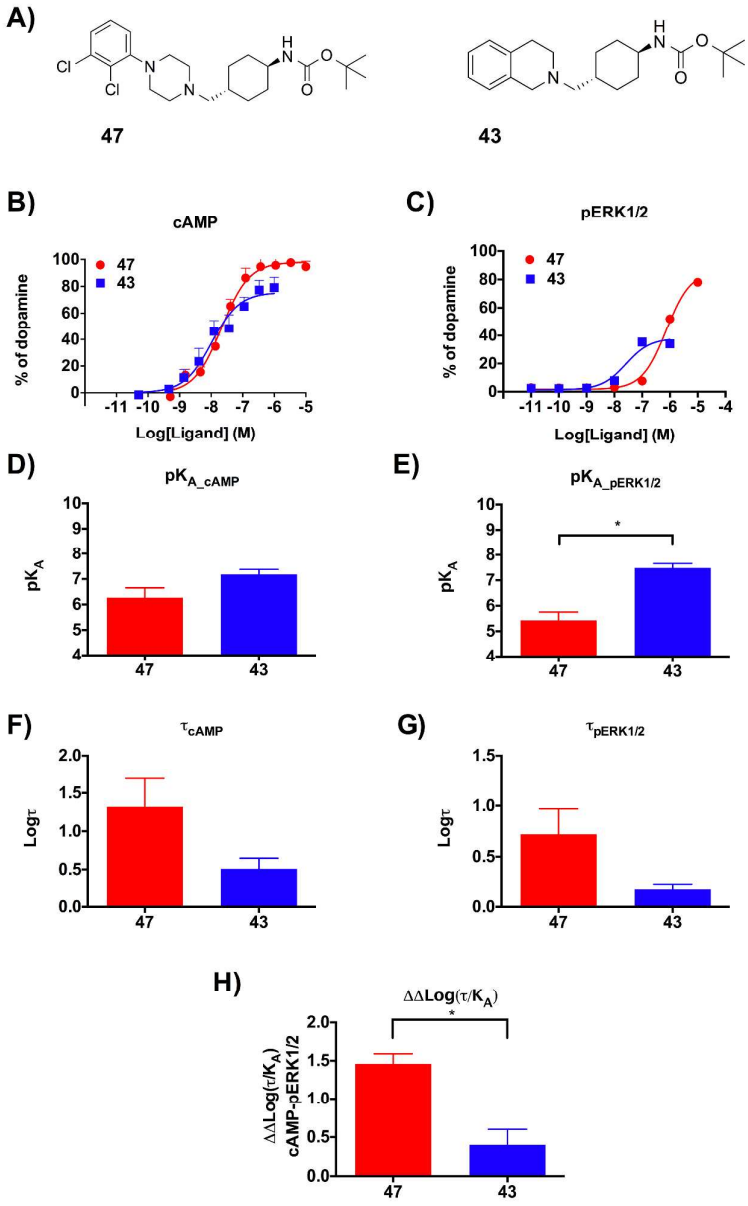

Figure 6: A) Modification of the 2,3-DCPP head group of **47**, to the THIQ head group (**43**) maintains (B) potency; (D) functional affinity; and (F) efficacy in an assay measuring inhibition of forskolin stimulated cAMP. In contrast this modification caused a significant increase in functional affinity at the pERK1/2 assay (C, E and G). As such, this modification confers significant biased agonism towards the pERK1/2 pathway (H).

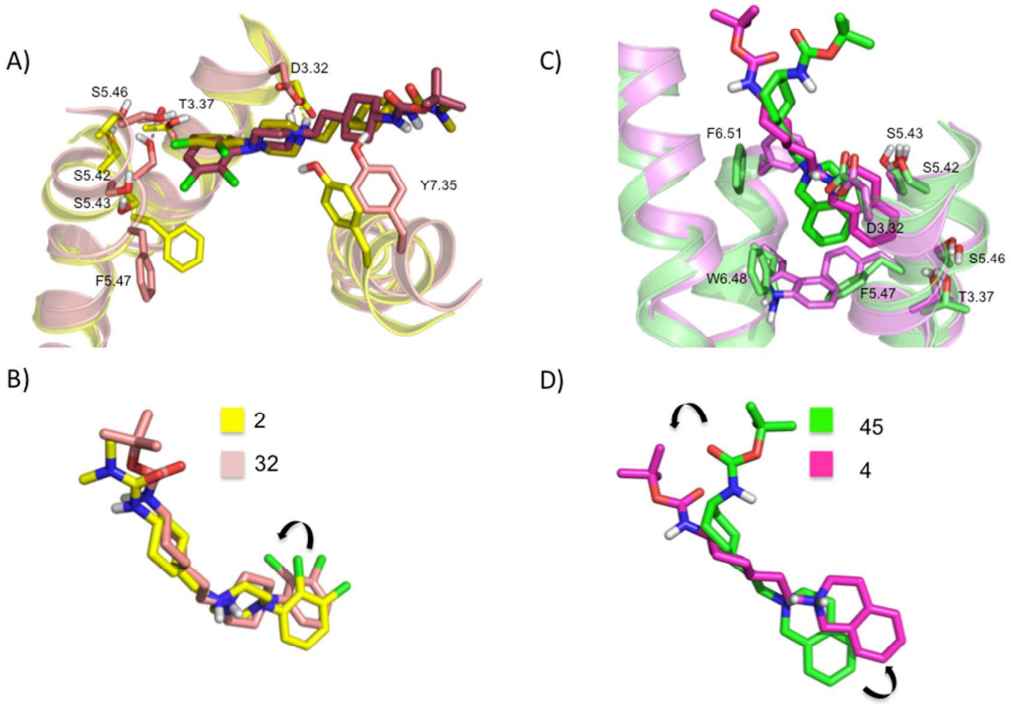

Figure 7: Superimposition of D_2R homology models in complex with compounds **2**, **32** (A,B) and **4**, **45** (C,D). A) Superimposition of models with either **2** (yellow) or **32** (pink) docked reveal that the orientation of the tail group is similar for both ligands. In contrast the 2,3-DCPP core adopts distinct orientations within the orthosteric site (A & B). Movement of residues within TM5, TM3 and TM7, including the conserved Ser5.42, Ser5.46 and Ser5.47, accompany these distinct orientations. In contrast, comparison of ligand-receptor interactions for **4** (purple) and the *cis* stereoisomer (**45**, green) reveal that both the tail and head groups adopt distinct orientations (C & D). Of note, a large movement of the highly conserved tryptophan within TM6 (Trp6.48) is observed between the two structures.

Table 1: List of compounds with variations to the tail region. Binding affinity, functional data in pERK1/2 and cAMP assays, and calculated bias are displayed for each compound.

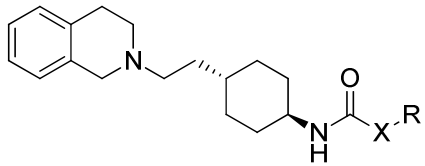

				pERK1/2				cAMP				pERK1/2-cAMP
compd	**X**	**R**	**pK_i**	**pK_A**	**Logτ**	**Log(τ/K_A)**	**ΔLog(τ/K_A)**	**pK_A**	**Logτ**	**Log(τ/K_A)**	**ΔLog(τ/K_A)**	**ΔΔLog(τ/K_A)**
DA	-	-	-	-	-	8.55 ± 0.04	0	-	-	8.55 ± 0.08	0	0
4	O	*t*-Bu	6.13 ± 0.15	7.10 ± 0.21#	-0.55 ± 0.06	6.54 ± 0.20	-2.01 ± 0.20	6.45 ± 0.20	0.56 ± 0.14	7.06 ± 0.11	-1.49 ± 0.20	0.51 ± 0.23
35	Me	-	5.22 ± 0.13	ND	ND	ND	ND	6.85 ± 0.36	-0.27 ± 0.10*	6.54 ± 0.35	-2.01 ± 0.36	-
37	O	Et	5.57 ± 0.17	ND	ND	ND	ND	7.23 ± 0.22^	-0.14 ± 0.08*	7.12 ± 0.19	-1.43 ± 0.19	-
38	O	*i*-Pr	5.83 ± 0.08	ND	ND	ND	ND	6.30 ± 0.24	-0.04 ± 0.11*	6.29 ± 0.18*	-2.26 ± 0.18*	-
39	O	*i*-Bu	5.28 ± 0.18*	ND	ND	ND	ND	6.05 ± 0.22	0.31 ± 0.13	6.40 ± 0.14*	-2.15± 0.14*	-
40	O	Ph	6.04 ± 0.23	ND	ND	ND	ND	5.67 ± 0.30	0.03 ± 0.16	5.72 ± 0.19*	-2.83 ± 0.19*	-
41	NMe	Me	6.00 ± 0.10	ND	ND	ND	ND	7.19 ± 0.20^	0.18 ± 0.10	7.40 ± 0.15	-1.15 ± 0.15	-
42	NH	*t*-Bu	6.61 ± 0.19	ND	ND	ND	ND	6.72 ± 0.32	-0.20 ± 0.09*	6.51 ± 0.31	-2.04 ± 0.32	-

DA = dopamine, ND = no agonist activity detected. Significant differences of parameter values from those of **4** are shown by * (one-way ANOVA, with Tukey post-test, $P < 0.05$).
pK_A values significantly different from pK_i values are shown by # (one-way ANOVA with Tukey post-test), $p < 0.05$) if values obtained in three assays or ^ (unpaired two-tailed Student's t-test, $p < 0.05$) if values only obtained for two assays.

Table 2: List of compounds with variations to the spacer region. Binding affinity, functional data in pERK1/2 and cAMP assays, and calculated bias are displayed for each compound.

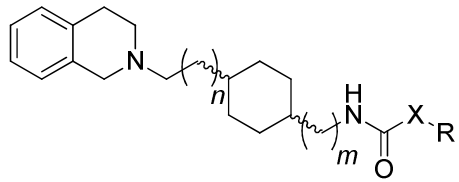

							pERK1/2				cAMP				cAMP-pERK1/2
compd	**Spacer**	***n***	***m***	**X**	**R**	**p*K*$_i$**	**p*K*$_A$**	**Log*τ***	**Log(*τ*/*K*$_A$)**	**ΔLog(*τ*/*K*$_A$)**	**p*K*$_A$**	**Log*τ***	**Log(*τ*/*K*$_A$)**	**ΔLog(*τ*/*K*$_A$)**	**ΔΔLog(*τ*/*K*$_A$)**
DA	-	-	-	-	-	-	-	-	8.55 ± 0.04	0	-	-	8.55 ± 0.08	0	0
4	*trans*	1	0	O	*t*-Bu	6.13 ± 0.15	7.10 ± 0.21#	-0.55 ± 0.06	6.54 ± 0.20	-2.01 ± 0.20	6.45 ± 0.20	0.56 ± 0.14	7.06 ± 0.11	-1.49 ± 0.20	0.51 ± 0.23
41	*trans*	1	0	NMe	Me	6.00 ± 0.10	ND	ND	ND	ND	7.19 ± 0.20^	0.18 ± 0.10	7.40 ± 0.15	-1.15 ± 0.15	-
43	*trans*	0	0	O	*t*-Bu	6.45 ± 0.19	7.48 ± 0.18#	0.17 ± 0.05*	7.32 ± 0.16	-1.23 ± 0.16	7.18 ± 0.2	0.51 ± 0.14	7.72 ± 0.12*	-0.83 ± 0.12*	0.40 ± 0.20
44	*trans*	0	1	O	*t*-Bu	5.94 ± 0.07	6.69 ± 0.75	-0.99 ± 0.19*	5.70 ± 0.65	-2.85 ± 0.65	6.82 ± 0.2	0.23 ± 0.10	7.09 ± 0.15	-1.46 ± 0.15	1.39 ± 0.66
45	*cis*	1	0	O	*t*-Bu	5.97 ± 0.17	ND	ND	ND	ND	7.34 ± 0.18*^	0.33 ± 0.10	7.70 ± 0.13*	-0.85 ± 0.13*	-
46	aromatic	1	0	O	*t*-Bu	6.26 ± 0.11	ND	ND	ND	ND	5.95 ± 0.26	-0.08 ± 0.27*	5.89 ± 0.19*	-2.66 ± 0.19*	-
54	*cis*	1	0	NMe	Me	4.87 ± 0.13*	ND	ND	ND	ND	6.96 ± 0.18^	0.34 ± 0.10	7.33 ± 0.12	-1.22 ± 0.12	-

DA = dopamine, ND = no agonist activity detected. Significant differences of parameter values from those of **4** are shown by * (one-way ANOVA, with Tukey post-test, $P < 0.05$).
p*K*$_A$ values significantly different from p*K*$_i$ values are shown by # (one-way ANOVA with Tukey post-test), $p < 0.05$) if values obtained in three assays or ^ (unpaired two-tailed Student's t-test, $p < 0.05$) if values only obtained for two assays.

Table 3: List of compounds with variations to the head group. Binding affinity, functional data in pERK1/2 and cAMP assays, and calculated bias are displayed for each compound.

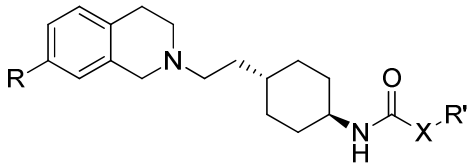

					pERK1/2				cAMP				cAMP-pERK1/2
Compd	**R**	**X**	**R′**	**pK_i**	**pK_A**	**Logτ**	**Log(τ/K_A)**	**ΔLog(τ/K_A)**	**pK_A**	**Logτ**	**Log(τ/K_A)**	**ΔLog(τ/K_A)**	**ΔΔLog(τ/K_A)**
DA	-	-	-	-	-	-	8.55 ± 0.04	0	-	-	8.55 ± 0.08	0	0
4	H	O	*t*-Bu	6.13 ± 0.15	7.10 ± 0.21	-0.55 ± 0.06	6.54 ± 0.20	-2.01 ± 0.20	6.45 ± 0.20	0.56 ± 0.14	7.06 ± 0.11	-1.49 ± 0.20	0.51 ± 0.23
29	NO_2	O	*t*-Bu	6.42 ± 0.24	ND	ND	ND	ND	ND	ND	ND	ND	-
30	CN	O	*t*-Bu	5.65 ± 0.16	ND	ND	ND	ND	6.81 ± 0.27	-0.01 ± 0.08*	6.82 ± 0.24	-1.73 ± 0.25	-
36	CN	Me	-	7.63 ± 0.12*	ND	ND	ND	ND	ND	ND	ND	ND	-

DA = dopamine, ND = no agonist activity detected. Significant differences of parameter values from those of **4** are shown by * (one-way ANOVA, with Tukey post-test, $P < 0.05$).
pK_A values significantly different from pK_i values are shown by # (one-way ANOVA with Tukey post-test), $p < 0.05$) if values obtained in three assays or ^ (unpaired two-tailed Student's t-test, $p < 0.05$) if values only obtained for two assays.

Table 4: List of compounds with 2,3-DCPP head group with variations to spacer and tail groups. Binding affinity, functional data in pERK1/2 and cAMP assays, and calculated bias are displayed for each compound.

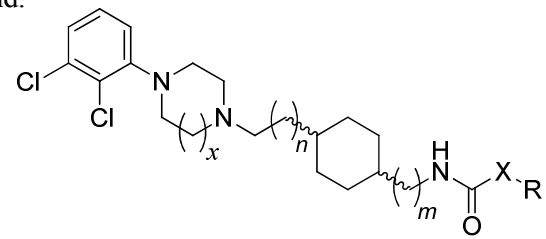

								pERK1/2				cAMP				cAMP-pERK1/2
Compd	**Spacer**	***x***	***n***	***m***	**X**	**R**	**p*K*$_i$**	**p*K*$_A$**	**Log*τ***	**Log(*τ*/*K*$_A$)**	**ΔLog(*τ*/*K*$_A$)**	**p*K*$_A$**	**Log*τ***	**Log(*τ*/*K*$_A$)**	**ΔLog(*τ*/*K*$_A$)**	**ΔΔLog(*τ*/*K*$_A$)**
DA	-	-	-	-	-	-	-	-	-	8.55 ± 0.04	0	-	-	8.55 ± 0.08	0	0
2	*trans*	1	1	0	NMe	Me	7.75 ± 0.10	7.61 ± 0.19	-0.37 ± 0.11	7.25 ± 0.17	-1.30 ± 0.17	8.71 ± 0.24*#	0.85 ± 0.20	9.59 ± 0.10*	1.04 ± 0.10*	2.34 ± 0.20*
31	*trans*	2	1	0	O	*t*-Bu	7.98 ± 0.08*	ND	ND	ND	ND	ND	ND	ND	ND	-
32	*trans*	1	1	0	O	*t*-Bu	7.40 ± 0.09	7.51 ± 0.13	-0.31 ± 0.04	7.21 ± 0.13	-1.34 ± 0.13	7.11 ± 0.28	0.76 ± 0.21	7.92 ± 0.11	-0.63 ± 0.11	0.71 ± 0.17
47	*trans*	1	0	0	O	*t*-Bu	6.51 ± 0.07*	5.43 ± 0.32*^	0.72 ± 0.09*	6.15 ± 0.09*	-2.04 ± 0.09*	6.27 ± 0.38	1.32 ± 0.37	7.61 ± 0.09	-0.94 ± 0.09	1.46 ± 0.13*
48	*trans*	1	0	1	O	*t*-Bu	6.83 ± 0.09*	6.86 ± 0.63	-0.85 ± 0.09*	6.00 ± 0.56	-2.55 ± 0.56	6.95 ± 0.19	-0.01 ± 0.08*	6.96 ± 0.16*	-1.59 ± 0.16*	0.95 ± 0.59
49	*cis*	1	1	0	O	*t*-Bu	7.48 ± 0.09	6.79 ± 0.17	-0.17 ± 0.11	6.62 ± 0.14	-1.93 ± 0.14	6.73 ± 0.19#	0.55 ± 0.13	7.30 ± 0.11*	-1.25 ± 0.11*	0.68 ± 0.17
55	*trans*	1	0	1	NMe	Me	7.37 ± 0.14	7.56 ± 0.50	-0.77 ± 0.09*	6.80 ± 0.47	-1.75 ± 0.47	6.92 ± 0.18	0.28 ± 0.09	7.22 ± 0.14*	-1.33 ± 0.14*	0.42 ± 0.49
56	*cis*	1	1	0	NMe	Me	6.99 ± 0.28	ND	ND	ND	ND	6.98 ± 0.21	-0.06 ± 0.10	6.95 ± 0.17*	-1.60 ± 0.17*	-

DA = dopamine, ND = no agonist activity detected. Significant differences of parameter values from those of **32** are shown by * (one-way ANOVA, with Tukey post-test, $P < 0.05$). pK_A values significantly different from pK_i values are shown by # (one-way ANOVA with Tukey post-test), $p < 0.05$) if values obtained in three assays or ^ (unpaired two-tailed Student's t-test, $p < 0.05$) if values only obtained for two assays.

Supporting Information

Additional tables of pharmacological data are available free of charge via the Internet at http://pubs.acs.org.

Author Information

Corresponding Author

For B.C. phone: +61 3 9903 9556; E-mail Ben.Capuano@monash.edu; (J.R.L.) phone +61 3 9903 9095, e-mail Rob.Lane@monash.edu

Notes

# These authors contributed equally to this work.

The authors declare no competing financial interest.

Acknowledgements

This research was supported by Project Grant 1052304 and Project Grant 1011920 of the National Health and Medical Research Council (NHMRC), Discovery grant DP110100687 of the Australian Research Council (ARC), and Program Grant 519461 (NHMRC). JRL is a R.D. Wright Biomedical Career Development Fellow (1052304, NHMRC) and a Larkin's Fellow (Monash University, Australia). JS acknowledges an Australian Postgraduate Award. CKH acknowledges a Monash Graduate Scholarship.

Abbreviations

DA, dopamine; 2,3-DCPHP, 1-(2,3-dichlorophenyl)homopiperazine; 2,3-DCPP, 1-(2,3-dichlorophenyl)piperazine; CHO, Chinese Hamster Ovary; THIQ, 1,2,3,4-tetrahydroisoquinoline

References

1. Ma, P.; Zemmel, R. Value of novelty? *Nat. Rev. Drug Discov.* **2002,** *1*, 571-572.

2. Lagerstrom, M. C.; Schioth, H. B. Structural diversity of G protein-coupled receptors and significance for drug discovery. *Nat. Rev. Drug Discov.* **2008,** *7*, 339-357.

3. Stevens, R. C.; Cherezov, V.; Katritch, V.; Abagyan, R.; Kuhn, P.; Rosen, H.; Wuthrich, K. The GPCR Network: a large-scale collaboration to determine human GPCR structure and function. *Nat. Rev. Drug Discov.* **2013,** *12*, 25-34.

4. Stallaert, W.; Christopoulos, A.; Bouvier, M. Ligand functional selectivity and quantitative pharmacology at G protein-coupled receptors. *Expert Opin. Drug. Dis.* **2011,** *6*, 811-825.

5. Violin, J. D.; Lefkowitz, R. J. β-Arrestin-biased ligands at seven-transmembrane receptors. *Trends Pharmacol. Sci.* **2007,** *28*, 416-422.

6. Kenakin, T.; Christopoulos, A. Signalling bias in new drug discovery: detection, quantification and therapeutic impact. *Nat. Rev. Drug Discov.* **2013,** *12*, 205-216.

7. Kenakin, T. Functional selectivity and biased receptor signaling. *J. Pharmacol. Exp. Ther.* **2011,** *336*, 296-302.

8. Urban, J. D.; Clarke, W. P.; von Zastrow, M.; Nichols, D. E.; Kobilka, B.; Weinstein, H.; Javitch, J. A.; Roth, B. L.; Christopoulos, A.; Sexton, P. M.; Miller, K. J.; Spedding, M.; Mailman, R. B. Functional selectivity and classical concepts of quantitative pharmacology. *J. Pharmacol. Exp. Ther.* **2007,** *320*, 1-13.

9. Davis, K. L.; Kahn, R. S.; Ko, G.; Davidson, M. Dopamine in schizophrenia: A review and reconceptualization. *Am. J. Psychiatry* **1991,** *148*, 1474-1486.

10. Urban, J. D.; Vargas, G. A.; von Zastrow, M.; Mailman, R. B. Aripiprazole has functionally selective actions at dopamine D_2 receptor-mediated signaling pathways. *Neuropsychopharmacol.* **2007,** *32*, 67-77.

11. Allen, J. A.; Yost, J. M.; Setola, V.; Chen, X.; Sassano, M. F.; Chen, M.; Peterson, S.; Yadav, P. N.; Huang, X.-p.; Feng, B.; Jensen, N. H.; Che, X.; Bai, X.; Frye, S. V.; Wetsel, W. C.; Caron, M. G.; Javitch, J. A.; Roth, B. L.; Jin, J. Discovery of β-arrestin–biased dopamine D_2 ligands for probing signal transduction pathways essential for antipsychotic efficacy. *Proc. Natl. Acad. Sci. U. S. A.* **2011,** *108*, 18488-18493.

12. Ágai-Csongor, É.; Domány, G.; Nógrádi, K.; Galambos, J.; Vágó, I.; Keserű, G. M.; Greiner, I.; Laszlovszky, I.; Gere, A.; Schmidt, É.; Kiss, B.; Vastag, M.; Tihanyi, K.; Sághy, K.; Laszy, J.; Gyertyán, I.; Zájer-Balázs, M.; Gémesi, L.; Kapás, M.; Szombathelyi, Z. Discovery of cariprazine (RGH-188): A novel antipsychotic acting on dopamine D_3/D_2 receptors. *Bioorg. Med. Chem. Lett.* **2012,** *22*, 3437-3440.

13. Gyertyán, I.; Kiss, B.; Sághy, K.; Laszy, J.; Szabó, G.; Szabados, T.; Gémesi, L. I.; Pásztor, G.; Zájer-Balázs, M.; Kapás, M.; Csongor, É. Á.; Domány, G.; Tihanyi, K.; Szombathelyi, Z. Cariprazine (RGH-188), a potent D_3/D_2 dopamine receptor partial agonist, binds to dopamine D_3 receptors in vivo and shows antipsychotic-like and procognitive effects in rodents. *Neurochem. Int.* **2011,** *59*, 925-935.

14. Kiss, B.; Horváth, A.; Némethy, Z.; Schmidt, É.; Laszlovszky, I.; Bugovics, G.; Fazekas, K.; Hornok, K.; Orosz, S.; Gyertyán, I.; Ágai-Csongor, É.; Domány, G.; Tihanyi, K.; Adham, N.; Szombathelyi, Z. Cariprazine (RGH-188), a dopamine D_3 receptor-preferring, D_3/D_2 dopamine receptor antagonist–partial agonist antipsychotic candidate: in vitro and neurochemical profile. *J. Pharmacol. Exp. Ther.* **2010,** *333*, 328-340.

15. Stemp, G.; Ashmeade, T.; Branch, C. L.; Hadley, M. S.; Hunter, A. J.; Johnson, C. N.; Nash, D. J.; Thewlis, K. M.; Vong, A. K. K.; Austin, N. E.; Jeffrey, P.; Avenell, K. Y.; Boyfield, I.; Hagan, J. J.; Middlemiss, D. N.; Reavill, C.; Riley, G. J.; Routledge, C.; Wood, M. Design and synthesis of

trans-N-[4-[2-(6-cyano-1,2,3,4-tetrahydroisoquinolin-2-yl)ethyl]cyclohexyl]-4-quinolinecarboxamide (SB-277011): a potent and selective dopamine D_3 receptor antagonist with high oral bioavailability and CNS penetration in the rat. *J. Med. Chem.* **2000,** *43*, 1878-1885.

16. Branch, C. L.; Johnson, C. N.; Stemp, G. (SmithKlineBeecham P.L.C., GB). Preparation of N-[2-(4-carboxamidocyclohexyl)ethyl]tetrahydroisoquinolines as dopamine D_3 receptor ligands. WO 98/50364 A1, November 12, 1998.

17. Branch, C. L.; Johnson, C. N.; Stemp, G. (SmithKlineBeecham P.L.C., GB). Preparation of tetrahydroisoquinolines as modulators of dopamine D_3 receptors. WO 99/64412 A1, December 16, 1999.

18. Silvano, E.; Millan, M. J.; la Cour, C. M.; Han, Y.; Duan, L.; Griffin, S. A.; Luedtke, R. R.; Aloisi, G.; Rossi, M.; Zazzeroni, F.; Javitch, J. A.; Maggio, R. The tetrahydroisoquinoline derivative SB269,652 is an allosteric antagonist at dopamine D_3 and D_2 receptors. *Mol. Pharmacol.* **2010,** *78*, 925-934.

19. Kenakin, T.; Watson, C.; Muniz-Medina, V.; Christopoulos, A.; Novick, S. A simple method for quantifying functional selectivity and agonist bias. *ACS Chem. Neurosci.* **2011,** *3*, 193-203.

20. Rajagopal, S.; Ahn, S.; Rominger, D. H.; Gowen-MacDonald, W.; Lam, C. M.; DeWire, S. M.; Violin, J. D.; Lefkowitz, R. J. Quantifying ligand bias at seven-transmembrane receptors. *Mol. Pharmacol.* **2011,** *80*, 367-377.

21. Black, J. W.; Leff, P. Operational models of pharmacological agonism. *Proc. R. Soc. Lond. B. Biol. Sci.* **1983,** *220*, 141-162.

22. Lane, J. R.; Sexton, P. M.; Christopoulos, A. Bridging the gap: bitopic ligands of G-protein-coupled receptors. *Trends Pharmacol. Sci.* **2013,** *34*, 59-66.

23. Bock, A.; Merten, N.; Schrage, R.; Dallanoce, C.; Batz, J.; Klockner, J.; Schmitz, J.; Matera, C.; Simon, K.; Kebig, A.; Peters, L.; Muller, A.; Schrobang-Ley, J.; Trankle, C.; Hoffmann, C.; De

Amici, M.; Holzgrabe, U.; Kostenis, E.; Mohr, K. The allosteric vestibule of a seven transmembrane helical receptor controls G-protein coupling. *Nat. Commun.* **2012,** *3*, 1-11.

24. Warne, T.; Moukhametzianov, R.; Baker, J. G.; Nehme, R.; Edwards, P. C.; Leslie, A. G. W.; Schertler, G. F. X.; Tate, C. G. The structural basis for agonist and partial agonist action on a β_1-adrenergic receptor. *Nature* **2011,** *469*, 241-244.

25. Rasmussen, S. G. F.; Choi, H.-J.; Fung, J. J.; Pardon, E.; Casarosa, P.; Chae, P. S.; DeVree, B. T.; Rosenbaum, D. M.; Thian, F. S.; Kobilka, T. S.; Schnapp, A.; Konetzki, I.; Sunahara, R. K.; Gellman, S. H.; Pautsch, A.; Steyaert, J.; Weis, W. I.; Kobilka, B. K. Structure of a nanobody-stabilized active state of the β_2 adrenoceptor. *Nature* **2011,** *469*, 175-180.

26. Rosenbaum, D. M.; Rasmussen, S. G. F.; Kobilka, B. K. The structure and function of G-protein-coupled receptors. *Nature* **2009,** *459*, 356-363.

27. Rosenbaum, D. M.; Cherezov, V.; Hanson, M. A.; Rasmussen, S. G. F.; Thian, F. S.; Kobilka, T. S.; Choi, H.-J.; Yao, X.-J.; Weis, W. I.; Stevens, R. C.; Kobilka, B. K. GPCR Engineering Yields High-Resolution Structural Insights into β_2-Adrenergic Receptor Function. *Science* **2007,** *318*, 1266-1273.

28. Swaminath, G.; Deupi, X.; Lee, T. W.; Zhu, W.; Thian, F. S.; Kobilka, T. S.; Kobilka, B. Probing the β_2 adrenoceptor binding site with catechol reveals differences in binding and activation by agonists and partial agonists. *J. Biol. Chem.* **2005,** *280*, 22165-22171.

29. Hiller, C.; Kling, R. C.; Heinemann, F. W.; Meyer, K.; Hübner, H.; Gmeiner, P. Functionally selective dopamine D_2/D_3 receptor agonists comprising an enyne moiety. *J. Med. Chem.* **2013,** *56*, 5130-5141.

30. Chen, X.; Sassano, M. F.; Zheng, L.; Setola, V.; Chen, M.; Bai, X.; Frye, S. V.; Wetsel, W. C.; Roth, B. L.; Jin, J. Structure–functional selectivity relationship studies of β-arrestin-biased dopamine D_2 receptor agonists. *J. Med. Chem.* **2012,** *55*, 7141-7153.

31. Fowler, J. C.; Bhattacharya, S.; Urban, J. D.; Vaidehi, N.; Mailman, R. B. Receptor conformations involved in dopamine D_{2L} receptor functional selectivity induced by selected transmembrane 5 serine mutations. *Mol. Pharmacol.* **2012,** *81*, 820-831.

32. Tschammer, N.; Bollinger, S.; Kenakin, T.; Gmeiner, P. Histidine 6.55 is a major determinant of ligand-biased signaling in dopamine D_{2L} receptor. *Mol. Pharmacol.* **2011,** *79*, 575-585.

33. Gay, E. A.; Urban, J. D.; Nichols, D. E.; Oxford, G. S.; Mailman, R. B. Functional selectivity of D_2 receptor ligands in a chinese hamster ovary *h*D_{2L} cell line: evidence for induction of ligand-specific receptor states. *Mol. Pharmacol.* **2004,** *66*, 97-105.

34. Tschammer, N.; Elsner, J.; Goetz, A.; Ehrlich, K.; Schuster, S.; Ruberg, M.; Ku□hhorn, J.; Thompson, D.; Whistler, J.; Hu□bner, H.; Gmeiner, P. Highly Potent 5-Aminotetrahydropyrazolopyridines: Enantioselective Dopamine D_3 Receptor Binding, Functional Selectivity, and Analysis of Receptor−Ligand Interactions. *J. Med. Chem.* **2011,** *54*, 2477-2491.

35. Newman, A. H.; Beuming, T.; Banala, A.; Donthamsetti, P.; Pongetti, K.; LaBounty, A.; Levy, B.; Cao, J.; Michino, M.; Luedtke, R.; Javitch, J. A.; Shi, L. Molecular determinants of selectivity and efficacy at the dopamine D_3 receptor. *J. Med. Chem.* **2012,** *55*, 6689-6699.

36. Roberts, D. J.; Lin, H.; Strange, P. G. Investigation of the mechanism of agonist and inverse agonist action at D_2 dopamine receptors. *Biochem. Pharmacol.* **2004,** *67*, 1657-1665.

37. Gottlieb, H. E.; Kotlyar, V.; Nudelman, A. NMR chemical shifts of common laboratory solvents as trace impurities. *J. Org. Chem.* **1997,** *62*, 7512-7515.

38. Mathe, T. B.; Hegedus, L.; Czibula, L.; Juhasz, B.; Nagy, B. J.; Markos, D. (Richter Gedeon NYRT, HU). A process for the preparation of *trans* aminocyclohexylacetic acid ethyl ester HCl. WO 2010/070368 A1, June 24, 2010.

39. Wustrow, D.; Belliotti, T.; Glase, S.; Kesten, S. R.; Johnson, D.; Colbry, N.; Rubin, R.; Blackburn, A.; Akunne, H.; Corbin, A.; Davis, M. D.; Georgic, L.; Whetzel, S.; Zoski, K.; Heffner,

T.; Pugsley, T.; Wise, L. Aminopyrimidines with high affinity for both serotonin and dopamine receptors. *J. Med. Chem.* **1998,** *41*, 760-771.

40. Villani, F. J.; Ellis, C. A. 4-Dimethylaminodi(2-thienyl)cyclohexylcarbinol and related compounds. *J. Org. Chem.* **1964,** *29*, 2585-2587.

41. Takita, H.; Noda, S.; Mukaida, Y.; Kobayashi, H. 4-(Aminomethyl)cyclohexane-1-carboxylic acid derivatives. EP 55145 A1, June 30, 1982.

42. Gobbi, L.; Jaeschke, G.; Luebbers, T.; Roche, O.; Rodriguez, S. R. M.; Steward, L. (F. Hoffmann-La Roche AG, CH). Benzoyl-piperidine derivatives as $5HT_2/D_3$ modulators and their preparation, pharmaceutical compositions and use in the treatment of CNS disorders. WO 2007/093540 A1, August 23, 2007.

43. Ozaki, F.; Ishibashi, K.; Ikuta, H.; Ishihara, H.; Souda, S. (Eisai Co., Ltd., JP). Preparation of anthranilic acid amide derivative as cyclic guanosine monophosphate-phosphodiesterase inhibitors. WO 95/18097 A1, July 6, 1995.

44. Cutrona, K. J.; Sanderson, P. E. J. The synthesis of thrombin inhibitor L-370,518 via an α-hydroxy-β-lactam. *Tetrahedron Lett.* **1996,** *37*, 5045-5048.

45. Joossens, J.; Van der Veken, P.; Lambeir, A. M.; Augustyns, K.; Haemers, A. Development of irreversible diphenyl phosphonate inhibitors for urokinase plasminogen activator. *J. Med. Chem.* **2004,** *47*, 2411-2413.

46. Lagisetti, C.; Pourpak, A.; Jiang, Q.; Cui, X.; Goronga, T.; Morris, S. W.; Webb, T. R. Antitumor compounds based on a natural product consensus pharmacophore. *J. Med. Chem.* **2008,** *51*, 6220-6224.

47. Ferber, E.; Bendix, H. 4-Aminocyclohexylacetic acid. *Ber. Dtsch. Chem. Ges. B* **1939,** *72B*, 839-848.

48. Hasumi, K.; Ohta, S.; Saito, T.; Sato, S.; Kato, J.-Y.; Sato, J.; Suzuki, H.; Asano, H.; Okada, M.; Matsumoto, Y.; Shirota, K. (Aska Pharmaceutical Co., Ltd., JP). Preparation of 5-amino-4-(4-pyrimidinyl)isoxazole derivatives as P38MAP kinase inhibitors and cytokine production inhibitors. WO 2006/070927 A1, July 6, 2006.

49. Grunewald, G. L.; Dahanukar, V. H.; Caldwell, T. M.; Criscione, K. R. Examination of the role of the acidic hydrogen in imparting selectivity of 7-(aminosulfonyl)-1,2,3,4-tetrahydroisoquinoline (SK&F 29661) toward inhibition of phenylethanolamine N-methyltransferase vs the α2-adrenoceptor. *J. Med. Chem.* **1997,** *40*, 3997-4005.

50. Agai-Csongor, E.; Galambos, J.; Nogradi, K.; Vago, I.; Gyertyan, I.; Kiss, B.; Laszlovszky, I.; Laszy, J.; Saghy, K. (Richter Gedeon Vegyeszeti Gyar RT., HU). A preparation of (thio)urea derivatives, useful as D_3/D_2 receptor antagonists. WO 2005/012266 A1, February 10, 2005.

51. Galambos, J.; Nogradi, K.; Againe, C. E.; Keseru, G. M.; Vago, I.; Domany, G.; Kiss, B.; Gyertyan, I.; Laszlovszky, I.; Laszy, J. (Richter Gedeon Vegyeszeti Gyar RT., HU). Preparation of *N*-[4-(2-heterocyclylethyl)cyclohexyl](hetero)arylsulfonamides as D_3 receptor agonists for treatment of CNS and ophthalmic disorders. WO 03/029233 A1, April 10, 2003.

52. Canals, M.; Lane, J. R.; Wen, A.; Scammells, P. J.; Sexton, P. M.; Christopoulos, A. A Monod-Wyman-Changeux mechanism can explain G Protein-coupled Receptor (GPCR) allosteric modulation. *J. Biol. Chem.* **2012,** *287*, 650-659.

53. Ballesteros, J. A.; Weinstein, H. Integrated methods for the construction of three-dimensional models and computational probing of structure-function relations in G protein-coupled receptors. In *Methods in Neurosciences*, Sealfon, S. C., Ed.; Academic Press: San Diego, 1995; Vol. 25, pp 366-428.

54. Thompson, J. D.; Gibson, T. J.; Plewniak, F.; Jeanmougin, F.; Higgins, D. G. The CLUSTAL_X windows interface: flexible strategies for multiple sequence alignment aided by quality analysis tools. *Nucleic Acids Res.* **1997,** *25*, 4876-4882.

55. Chien, E. Y. T.; Liu, W.; Zhao, Q.; Katritch, V.; Won Han, G.; Hanson, M. A.; Shi, L.; Newman, A. H.; Javitch, J. A.; Cherezov, V.; Stevens, R. C. Structure of the human dopamine D_3 receptor in complex with a D_2/D_3 selective antagonist. *Science* **2010,** *330*, 1091-1095.

56. Sali, A.; Blundell, T. L. Comparative protein modelling by satisfaction of spatial restraints. *J. Mol. Biol.* **1993,** *234*, 779-815.

57. Duan, Y.; Wu, C.; Chowdhury, S.; Lee, M. C.; Xiong, G.; Zhang, W.; Yang, R.; Cieplak, P.; Luo, R.; Lee, T.; Caldwell, J.; Wang, J.; Kollman, P. A point-charge force field for molecular mechanics simulations of proteins based on condensed-phase quantum mechanical calculations. *J. Comput. Chem.* **2003,** *24*, 1999-2012.

58. Wang, J.; Wolf, R. M.; Caldwell, J. W.; Kollman, P. A.; Case, D. A. Development and testing of a general amber force field. *J. Comput. Chem.* **2004,** *25*, 1157-1174.

59. Phillips, J. C.; Braun, R.; Wang, W.; Gumbart, J.; Tajkhorshid, E.; Villa, E.; Chipot, C.; Skeel, R. D.; Kalé, L.; Schulten, K. Scalable molecular dynamics with NAMD. *J. Comput. Chem.* **2005,** *26*, 1781-1802.

60. MacKerell Jr, A. D.; Bashford, D.; Bellott, M.; Dunbrack Jr, R. L.; Evanseck, J. D.; Field, M. J.; Fischer, S.; Gao, J.; Guo, H.; Ha, S.; Joseph-McCarthy, D.; Kuchnir, L.; Kuczera, K.; Lau, F. T. K.; Mattos, C.; Michnick, S.; Ngo, T.; Nguyen, D. T.; Prodhom, B.; Reiher III, W. E.; Roux, B.; Schlenkrich, M.; Smith, J. C.; Stote, R.; Straub, J.; Watanabe, M.; Wiórkiewicz-Kuczera, J.; Yin, D.; Karplus, M. All-atom empirical potential for molecular modeling and dynamics studies of proteins. *J. Phys. Chem. B* **1998,** *102*, 3586-3616.

61. Christopoulos, A. Assessing the distribution of parameters in models of ligand–receptor interaction: to log or not to log. *Trends Pharmacol. Sci.* **1998,** *19*, 351-357.

62. Leff, P.; Prentice, D. J.; Giles, H.; Martin, G. R.; Wood, J. Estimation of agonist affinity and efficacy by direct, operational model-fitting. *J. Pharmacol. Methods* **1990,** *23*, 225-237.

63. Motulsky, H. J.; Ransnas, L. A. Fitting curves to data using nonlinear regression: a practical and nonmathematical review. *The FASEB Journal* **1987,** *1*, 365-74.

Table of Contents graphic